

PART II SURVEY RESULTS

CHAPTER 1 EXISTING DATA ANALYSIS

For the existing data analysis, such existing data as geological literatures, geological maps, topographical maps and aerial photographs were collected, arranged and analyzed. To be concrete, existing information and data concerning the geological features, geological structure, mineral deposit and the result of geochemical prospecting of the project area was compiled and analyzed to understand the outline of geological features, geological structure, mineral deposit and potential ore fields.

In the survey area, gold ore deposits were recognized in greenstone and it is considered that the ore deposit is closely associated with granodiorites. Based on this information, the field survey area (about 2,500km²), where the greenstone belt had been distributed and many intrusions of granodiorites rock body had been recognized, was extracted from the project area (12,000 km²), according to the result of the existing data analysis and the geologic interpretation of satellite image data. The detail of the analysis is described in Part1-Chapter3, and the collected data is listed in the reference.

CHAPTER 2 GEOLOGIC INTERPRETAION OF SATELITE IMAGE DATA

2-1 Key objective

The key objective is to full understand the regional geologic structure of the survey area and to prepare the basic map for regional potential evaluation of the survey area as well as by photo-geologic interpretation of the satellite image.

2-2 Survey area

The survey area for geologic interpretation of the satellite image data covers both the San Jose and the Arroyo Grande Areas and the gross area amounts to 12,000km². The location of the survey area is indicated in Fig. II-2-1 along with the coverage of the satellite image.

2-3 Image data used

The image data used for this survey is listed in Tab. II-2-1.

2-4 Image product

The image products generated by this survey are listed in Tab. II-2-2.

2-4-1 Digital mosaicing

A digital mosaicing method was applied to JERS-1/SAR images and LANDSAT/TM data. The principal data processing procedures are recounted below. The acquired digital mosaic imagery of JERS-1/SAR is shown in Fig. II-2-2.

(1) JERS-1/SAR image data

- Bit conversion process

- Antenna pattern correction

- Noise reduction (median filter)

(2) LANDSAT/TM data

- Image inspection

(3) Both data in common

- Extraction of relative position information between images

- Contrast adjustment

- Image mosaic

- Contrast enhancement process

- Geometric conversion (UTM, Zone21, WGS84)

- Annotation

2-4-2 TM false color image

The band combination B:G:R = 1:4:5, which is adequate to define the survey area, was applied for the false color composition. Fig. II-2-3 shows the TM false color imagery processed.

2-4-3 TM band ratio image

The band rationing B:G:R = 3/1:5/4:5/7, which has been considered to be the most suitable for the discrimination of the alteration zone, was adopted for this false color composition. The color composed by each band rationing can be used to discriminate the following minerals. Fig. II-2-4 shows the TM band ratio imagery processed.

| Color | B=3/1 | G=5/4 | R=5/7 | Discriminating mineral |
|----------------|-------|-------|-------|------------------------|
| Red | △ | △ | ○ | Clay |
| Yellow ~ brown | △ | ○ | ○ | Clay + hematite |
| Green | △ | ○ | △ | Hematite |
| Green ~ blue | ○ | ○ | △ | Iron mineral |
| Blue | ○ | △ | △ | Iron mineral |
| Magenta | ○ | △ | ○ | Clay + iron mineral |
| White | ○ | ○ | ○ | Clay + iron mineral |

Note) ○: excellent potential to discriminate, △: medium to unlikely potential to discriminate

2-5 Contents of photo-geological interpretation

The interpretation of image data was performed, conforming to the photo-geological interpretation procedure, using a paper-printed image on a scale of 1:250,000. The reference factors of interpretation are color or tone on the screen, pattern and distribution density of drainage system, resistance to rock erosion, bedding or layering, vegetation and land-use. The existing geological map used to refer to the geologic units as a comparison, was the "Carta Geológica, produced by Ministerio de Industria y Energía (1980)" on a scale of 1:500,000. In addition, geological structure including lineament and alteration zone were also extracted.

2-6 Result of photo-geological interpretation

2-6-1 JERS-1/SAR image data

(1) Description of the image

The image data used was in good condition, but had the following features due to the relation between the L-band that the SAR in question had used, and the features of the targeted surface. The enhancement effect of topographic feature using geometric distortion of the SAR data is insufficient because the surface of the survey area is extremely flat.

Mosaic texture had appeared on the imagery corresponding to the variety and growth stages of crops

because the targeted area was widely used for cultivation. This was an obstacle to the geological interpretation.

Microwave was irradiated in the direction from east to west. As a result, the orthogonal roads with this direction and, electric cables and fences along the roads tend to be enhanced. Basically the drainage system is reasonably highlighted on the imagery. However there are some areas where the extraction of the primary drainage system is difficult. A part of the drainage system is expressed with strong luminance, which is considered due to an accumulation of arboret on the stream that has an influence on the optical reflection as well as a double reflection between the arboret and the water surface. Accordingly, existence of water is estimated in nearly all areas of the drainage system.

(2) Geologic interpretation

First, gneisses of Proterozoic (comparison geologic unit pCCcb series in the geological map on a scale of 1:500,000) and sedimentary rocks of post-Mesozoic (K, T and Q series in the same map) can be discriminated in terms of the distribution on the surface and land-use. The former is characterized by rolling topographical relief and developed drainage system, while the latter by terrace-like distribution on the platform, strong land-use and an undeveloped drainage system.

As for the gneisses of Proterozoic, further discrimination is difficult for the whole survey area. However gneiss pCCcp and other rocks including granites pCCG and pCC, and greenstone pCCps, which are comprised in the gneisses, can be discriminated in a specific area. Granites pCCG and pCC show rather rough topographic features being compared with gneiss pCCcb and greenstone pCCps, and their luminance tends to be strong on the screen. Gneiss pCCcb and greenstone pCCps shows very similar evidence. However, the latter can be traced by means of its bedded structure.

In general terms, greenstone pCCps is distributed both in the east and west part of the survey area. It is pointed out and expected that, there is a possibility of another unreported distribution lying midway between them. In the east of the survey area, discrimination between gneiss pCCcb and greenstone pCCps is difficult. However, it is considered that the distribution is almost the same as the existing geological map.

(3) Extraction of geological structure

In the south of the survey area, the faults are developed having two predominant trends of ENE-WSW and NW-SE. The former trending faults are older, and the latter divides them to form the survey area into a blocked structure in a NW-SW direction. Some of the granitic rocks (pCCG and pCC) are distributed in association with the ENE-WSW trending faults. The emplacement is estimated at approximately the same age as when the faults were formed. Lineament is developed with an intermediate density and demonstrates a tendency to have predominant trends NW-SE and NE-SW.

(4) Extraction of the alteration zone

In this imagery, the lineament density tends to be high around the old mines or mineral showings. However it is difficult to directly extract the alteration zone.

2-6-2 LANDSAT/TM data

Using the result of the above-mentioned JERS-1/SAR image data interpretation, the features of the image of the survey area were resumed on the TM imagery. The geological aspects are described below.

(1)Description of the image

The image data used was in good condition, and had the following features.

①The solar altitude and sun azimuth (clockwise from the north) at the time of taking the image, were 34° and 53° , respectively. As the survey area has a flat topographic feature, low solar altitude is better. The solar altitude at the winter solstice of the survey area is around 20° , and it provides good conditions. The sun azimuth generally has an oblique trend as against the geological trends of the survey area, and that presents suitable conditions for the geological interpretation.

②The topography of the survey area is generally flat. However minute relief is shown on the imagery and topographical feature and drainage system can be sufficiently extracted.

The surface of the targeted area was widely used for cultivation. This is an obstacle when the distinctive spectrums depending on rocks and soils are extracted in the area covered by vegetation.

(2)Geologic interpretation

The geologic interpretation map is shown in Fig. II-2-5, and the geologic interpretation chart is summarized in Tab. II-2-3 along with the interpretation result of JERS-1/SAR image. Features of each geologic unit are described below.

[Unit gn1]

This geologic unit manifests such features as magenta in color, dendritic pattern of the drainage system and extremely high drainage density. This unit is characterized by high resistance to rock erosion and rough texture. Bedding is developed in the unit and the degree of land-use is common. The unit is widely distributed in the whole survey area and compares with the gneiss of Proterozoic pCCcb.

[Unit g]

This geologic unit manifests such features as magenta in color, parallel pattern of the drainage system and extremely high drainage density. This unit is characterized by high resistance to rock erosion and lined texture. Bedding is developed in the unit and the degree of land-use is common. The unit is widely distributed both in the south part of the Arroyo Grande area and also the south part of the San Jose area and, compares with the gneiss of Proterozoic pCCG.

[Unit gs]

This geologic unit manifests such features as green and red patched color, sub-parallel pattern of the

drainage system and high drainage density. This unit is characterized by high resistance to rock erosion and lineated texture. Bedding is extremely well developed in the unit and the degree of land-use is strong. The unit is distributed both in the central part of the Arroyo Grande area, the central part of the San Jose area in a direction of E-W and compares with the greenstone of Proterozoic pCCps.pCCsj.

[Unit sh]

This geologic unit manifests such features as magenta in color, sub-dendritic pattern of the drainage system and high drainage density. This unit is characterized by intermediate resistance to rock erosion and rough texture. Bedding is developed in the unit and the degree of land-use is high. The unit is distributed in the south part of the Arroyo Grande area in a direction of E-W and compares with the gneisses of Proterozoic pCCApd.

[Unit gn2]

This geologic unit manifests such features as green and red patched color, sub-dendritic pattern of the drainage system and high drainage density. This unit is characterized by intermediate resistance to rock erosion and smooth texture. Bedding is moderately developed in the unit and the degree of land-use is high. The unit is distributed in the south part of the Arroyo Grande area in a direction of E-W and compares with the gneiss of Proterozoic pCCcb. This unit is differentiated from the Unit gn1, being bounded by the above-mentioned Unit g, Unit gs and Unit sh. In the southwest part of the Arroyo Grande area, there are some fields where the compartmentation of Unit g1 and Unit g2 is difficult.

[Unit Ka]

This geologic unit manifests such features as magenta in color, sub-parallel pattern of the drainage system and high drainage density. This unit is characterized by intermediate resistance to rock erosion and rough texture. Bedding is not developed well in the unit and vegetation is sparse. The unit is distributed in the southeast part of the Arroyo Grande area and compares with the sedimentary rocks of Cretaceous Ksm and Klal.

[Unit Kb]

This geologic unit manifests such features as green and red patched color, dendritic pattern of the drainage system and high drainage density. This unit is characterized by intermediate resistance to rock erosion and rough texture. Bedding is not well developed in the unit and the degree of land-use is high. The unit is distributed in the north part of the San Jose area and compares with the sedimentary rocks of Cretaceous Klm.

[Unit T-K]

This geologic unit manifests such features as green and red patched color, dendritic pattern of the drainage system and low drainage density. This unit is characterized by low resistance to rock erosion and flat terrace-like texture. Bedding is not well developed in the unit and the degree of land-use is high. The unit is distributed both in the west part of the Arroyo Grande area and the western part of the San Jose area and, compares with the sedimentary rocks of Cretaceous Ksa.

[Unit Q]

This geologic unit manifests such features as green and red patched color, dendritic pattern of the drainage system and low drainage density. This unit is characterized by low resistance to rock erosion and flat terrace-like texture. Bedding is not developed in the unit and the degree of land-use is high. The unit is distributed in the south part of the Arroyo Grande area and compares with the sedimentary layer of Quaternary Q1. The topographical feature is similar to the Unit T-K.

[Unit a]

This geologic unit manifests such features as black in color, braided pattern of the drainage system and low drainage density. This unit is characterized by extremely low resistance to rock erosion and even texture. The vegetation is dense and compares with the alluvial layer of Quaternary Q.

[Unit G]

This geologic unit manifests such features as purple in color, sub-dendritic pattern of the drainage system and extremely high drainage density. This unit is characterized by extremely high resistance to rock erosion and extremely rough texture. The topographical relief is rough in the even area, and land-use is hardly recognized. The unit intrudes throughout in the whole of the survey area and compares with the intrusive granitic rocks (pCCG, pCC).

(3) Extraction of geological structure

In the south of the survey area, the faults are developed having two predominant trends of ENE-WSW and NW-SE. The former trending faults are older, and the latter divides them to form the survey area into a blocked structure in a NW-SW direction. Some of the intrusive granitic rocks (pCCG and pCC: corresponding to the geologic unit G) are distributed in association with the ENE-WSW trending faults. The emplacement is estimated at approximately the same age as when the faults were formed.

The fold structure is small-scale, locally predominate in the domain structure, and is not a predominant structure in the whole area.

2-7 Result of lineament analysis

2-7-1 Extraction of lineament

Extraction of lineament was carried out by using both the JERS-SAR image data and LANDSAT/TM image data. In consequence of a comparison of both results, in the case of JERS-SAR image, many roads and boundaries between vegetation were misidentified as a lineament, and that seriously affected the accuracy. Accordingly, the final lineament map was completed, after each lineament extraction from the JERS-1/SAR image data was checked and verified one by one on the LANDSAT/TM imagery. Other lineament which was extracted only from the LANDSAT/TM imagery was also added. The result of the extraction of lineament is shown in Fig. II-2-6.

2-7-2 Lineament analysis

Generally, the lineament is developed without discriminating predominant trends, while the N-S

trending lineaments are developed in the east part of the Arroyo Grande area as well as the San Jose area. No lineament that has a predominant E-W trend is developed in any part of the area. The lineaments are densely found in the northern part of the Mahoma mine and form a high-density zone of ring arrangement. Lineament density is higher in the eastern part of the Arroyo Grande area, when compared with the other areas. The lineament density map is shown in Fig. II-2-6 along with the lineament extraction result.

2-8 Extraction of alteration zone

In this imagery, the lineament density tends to be high around the old mines or mineral showings. However it was difficult to directly extract the alteration zone. The ore deposit type expected in this survey area is gold ore deposit accompanying shear zone, which is generally subjected to mineralization of greenschist facies, and is also subjected to mineralization of amphibolite facies by contact metamorphism especially around the intrusive rock. Accordingly, depending on the wall rock composition, alteration zones of silicification and sericitization are usually targeted for extraction.

The color appeared on the TM band ratio image can largely be classified roughly into magenta and cyan. The former is a composite of blue and red, and provides a high pixel value of both bands rationing 3/1 and 5/7. This color suggests the existence of clay and goethite. However, it was not enough to extract the possible alteration zone because it is pervasive all over the survey area. The latter is a composite of blue and green, and provides a high pixel value of both bands rationing 3/1 and 5/4. This color suggests the existence of iron minerals. The color is pervasive all over the survey area and is also recognized in the geologic unit G. Although this color can determine the lithofacies, it was not enough to extract the possible alteration zone as in the former case.

2-9 Result of image analysis

Considering the expected ore deposit type, the potential of the ore bearing area analyzed at this stage, requires at least the following necessary conditions.

- ①Existence of faults developed in predominant trends ENE-WSW and NW-SE.
- ②It is situated in or near the area which Unit gs and Unit G are distributed.
- ③Lineament, which is considered to reflect the geological structure, is concentrated, although the scale range is different from the faults.

As for ①, it is considered that the faults as well as ③ provide space for ore deposits to lie. However, it is necessary to figure out the timing of activity in relation to Unit G. As for ② it is pointed that Unit gs is important as a supply source of hydrothermal solution, and Unit G as a heat source. Based on these aspect, the interpretation map of satellite imagery resuming the result of geological interpretation is shown in Fig. II-2-7. As a result, the following two areas can be appointed as the locations that fill all these requirements.

San Jose area

- ①Around the Mahoma mine

②The area about 20km west from the Mahoma mine

Arroyo Grande area

①Further west than the northwest part of the area

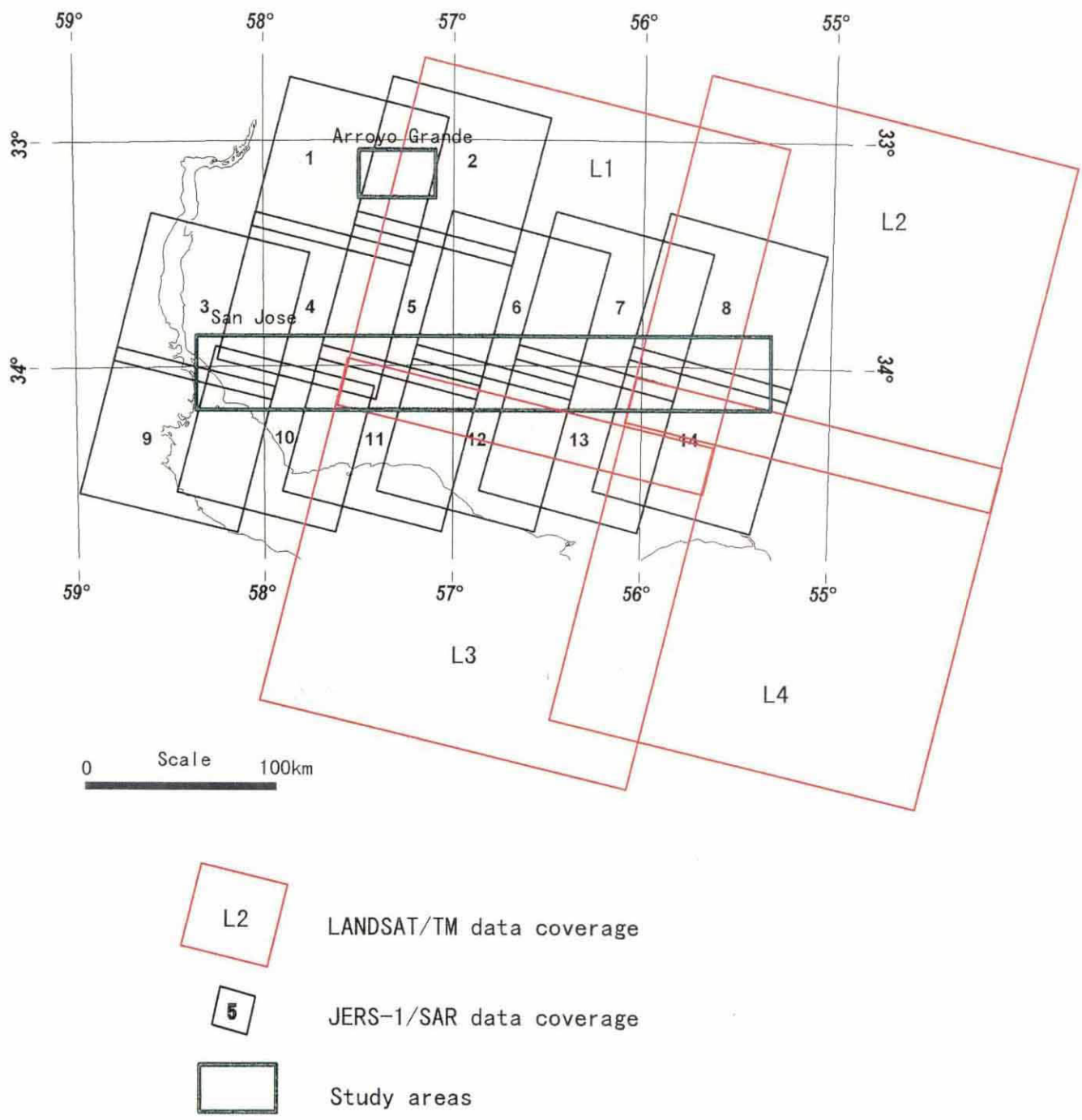


Fig.II-2-1 Coverage map of satellite imagery

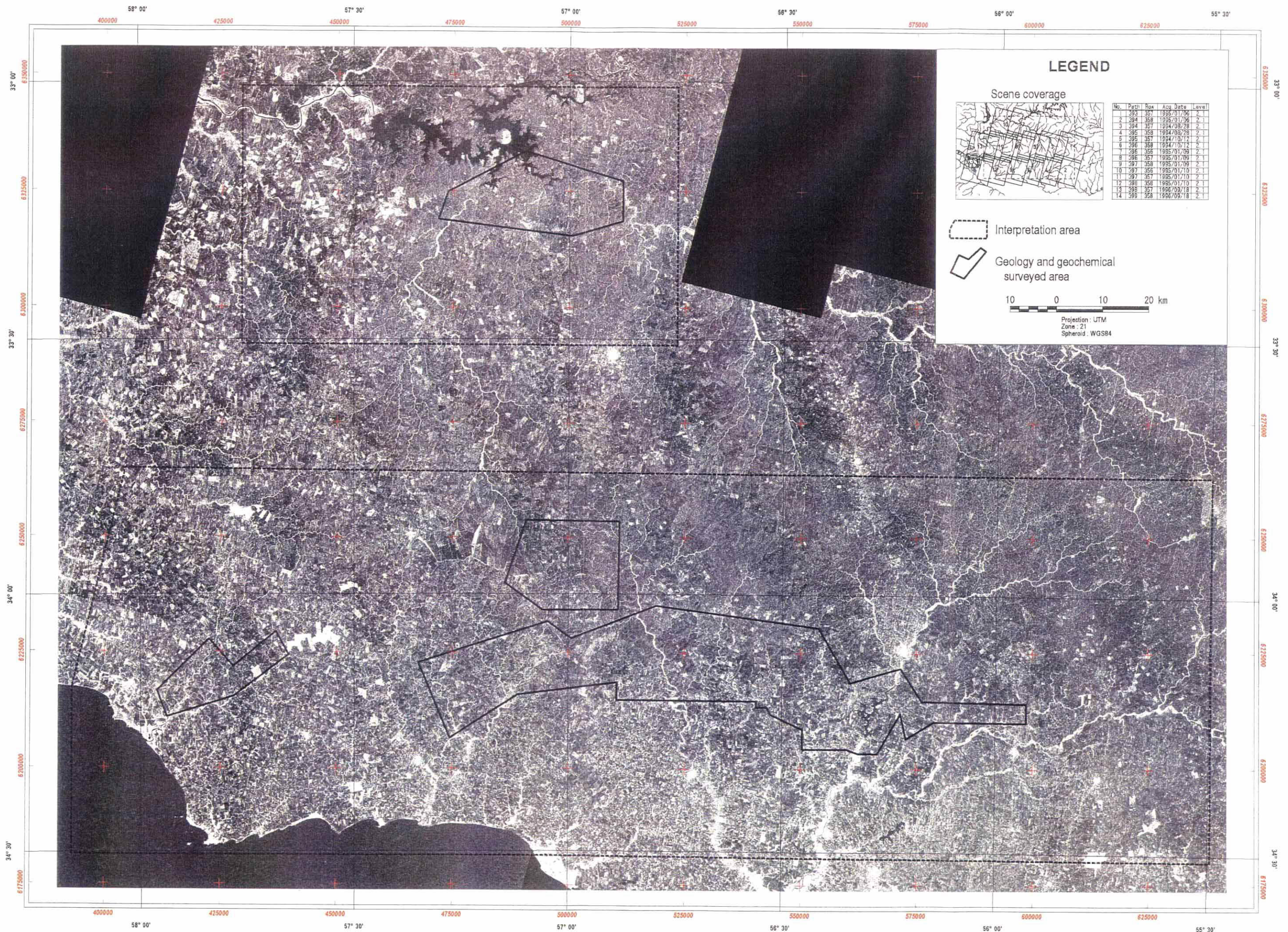


Fig.II-2-2 Digital mosaic of JERS-1/SAR imagery

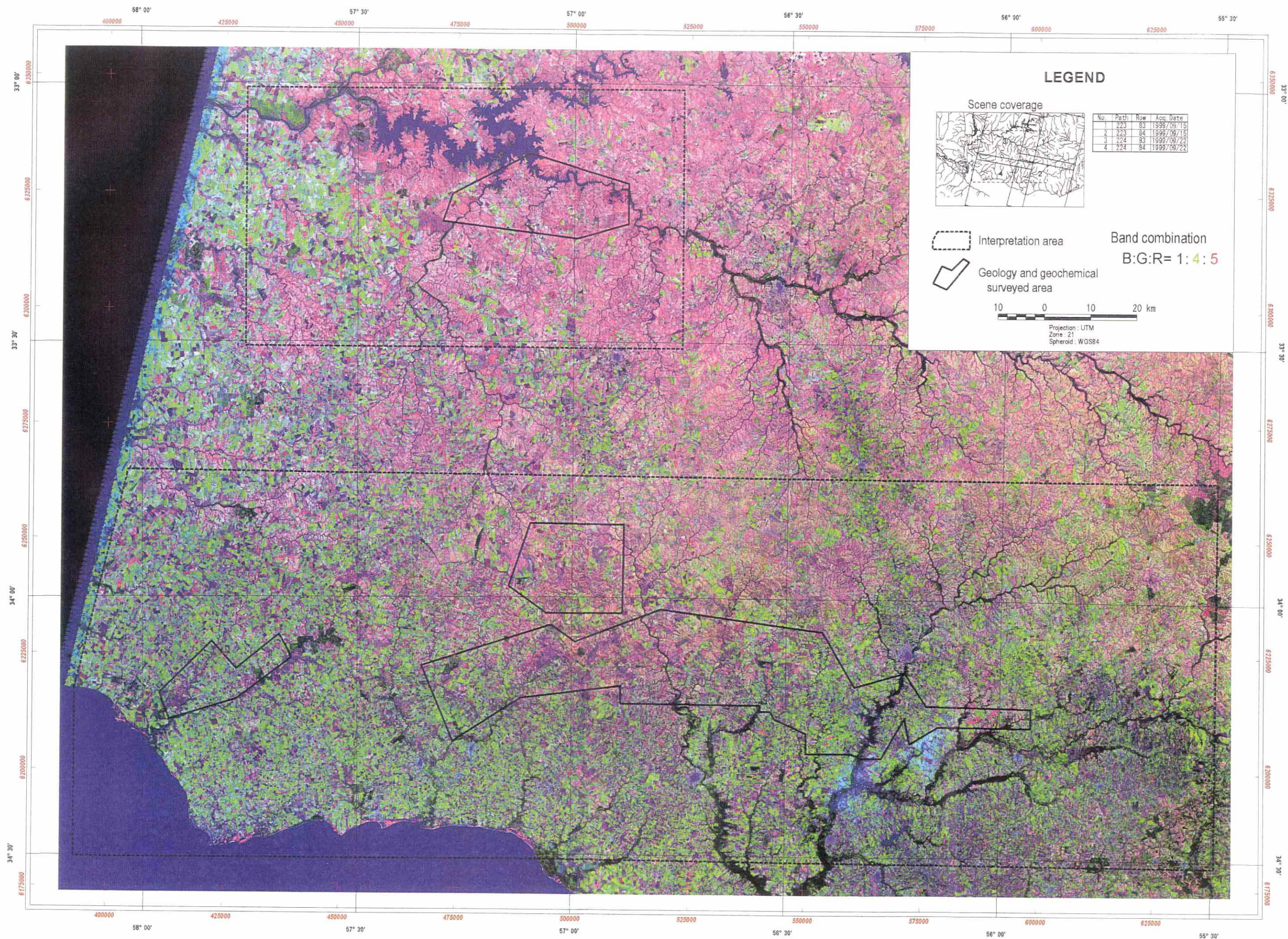


Fig.II-2-3 Digital mosaic of LANDSAT/TM imagery

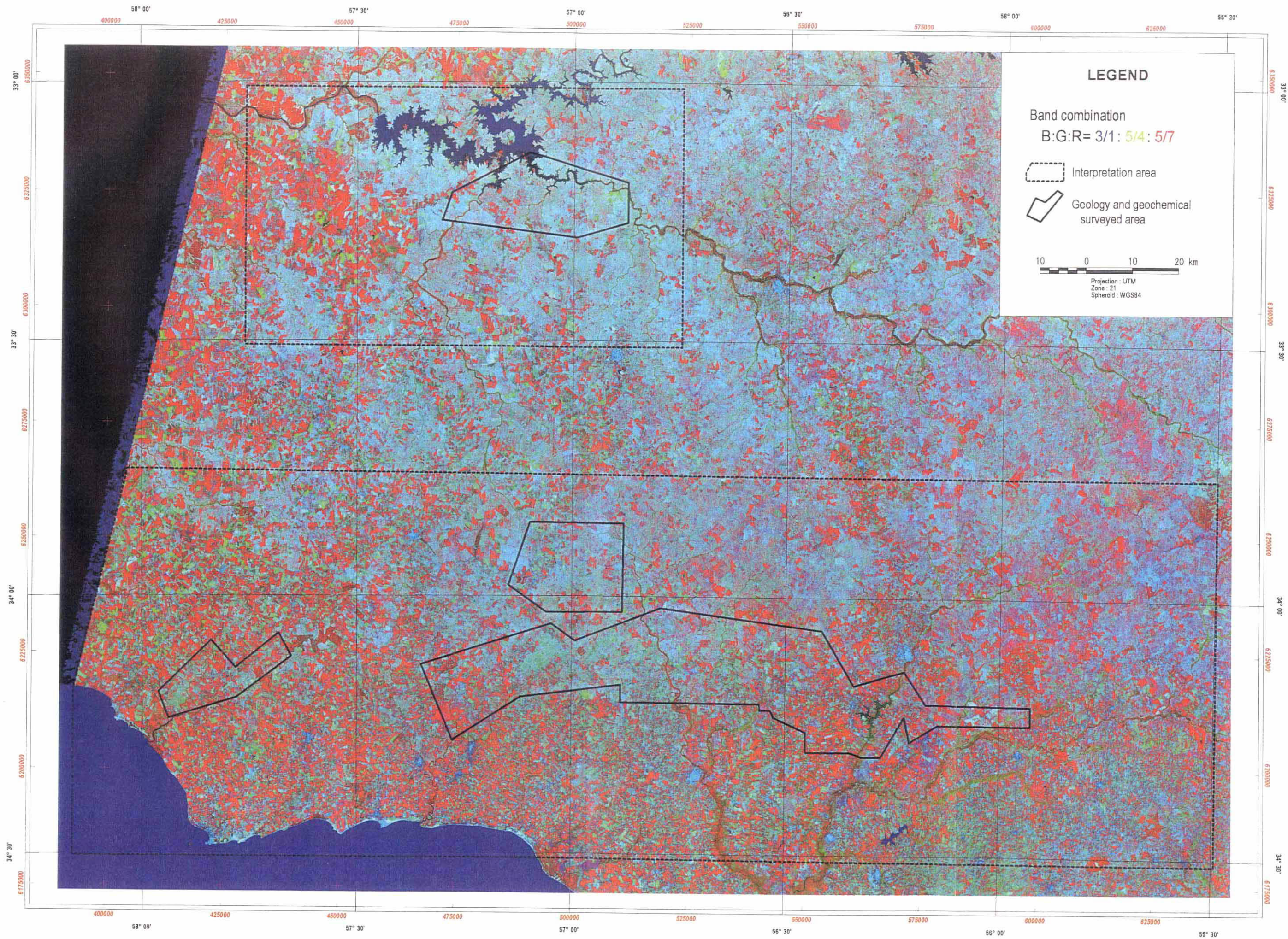


Fig.II-2-4 Band ratio imagery of LANDSAT/TM data

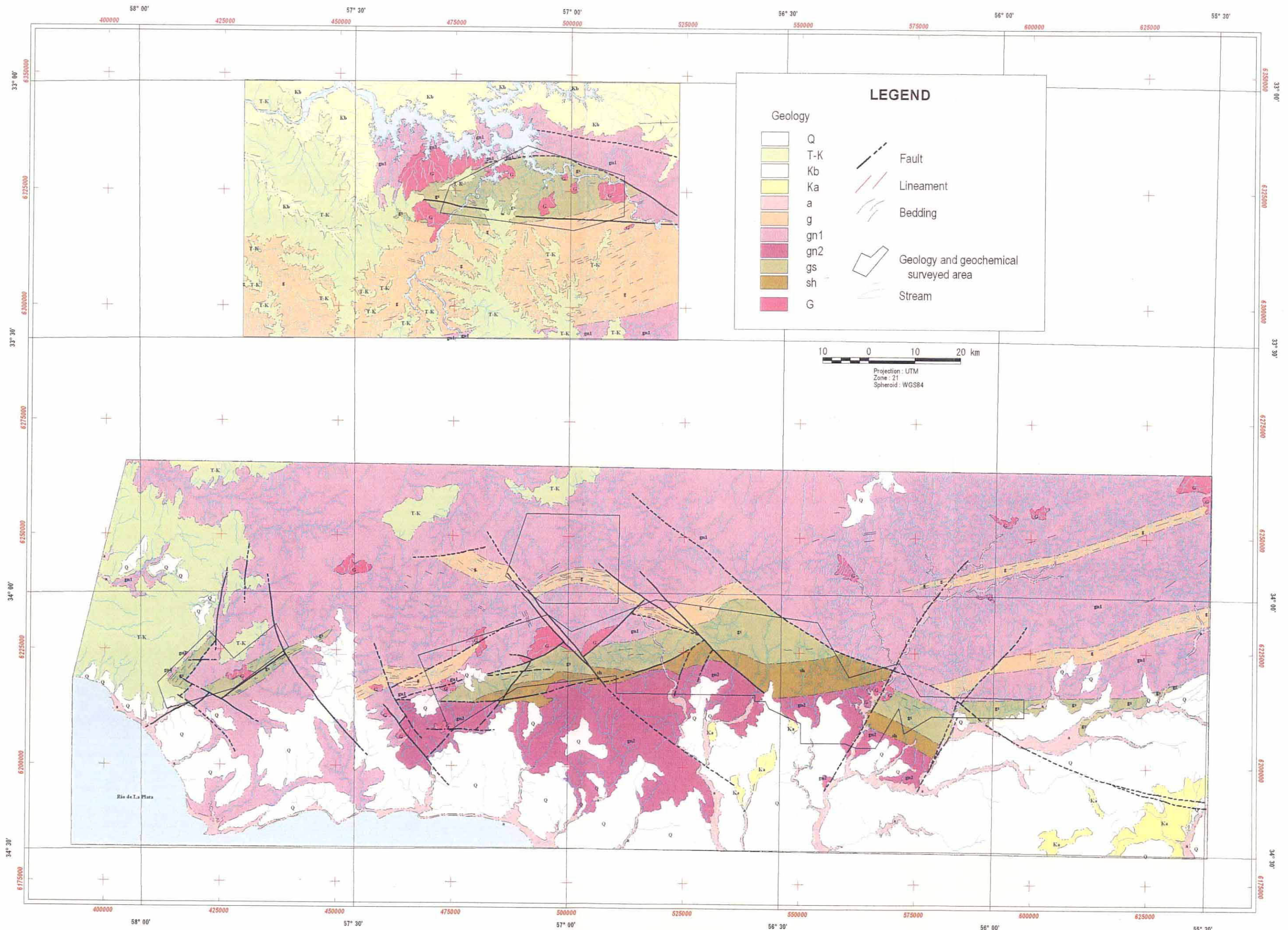


Fig.II-2-5 Geologic interpretation map

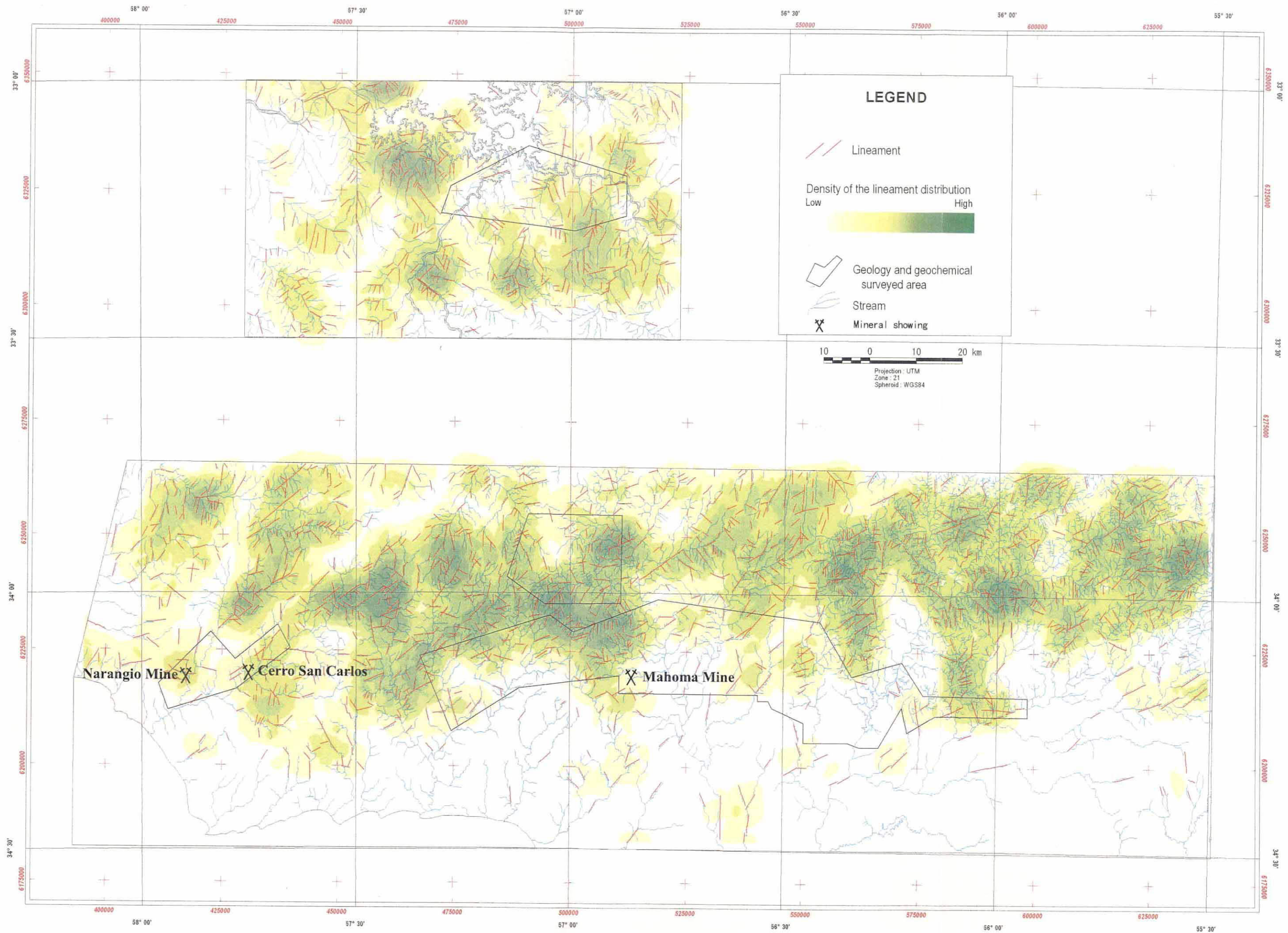


Fig. II-2-6 Lineament extraction and its density map

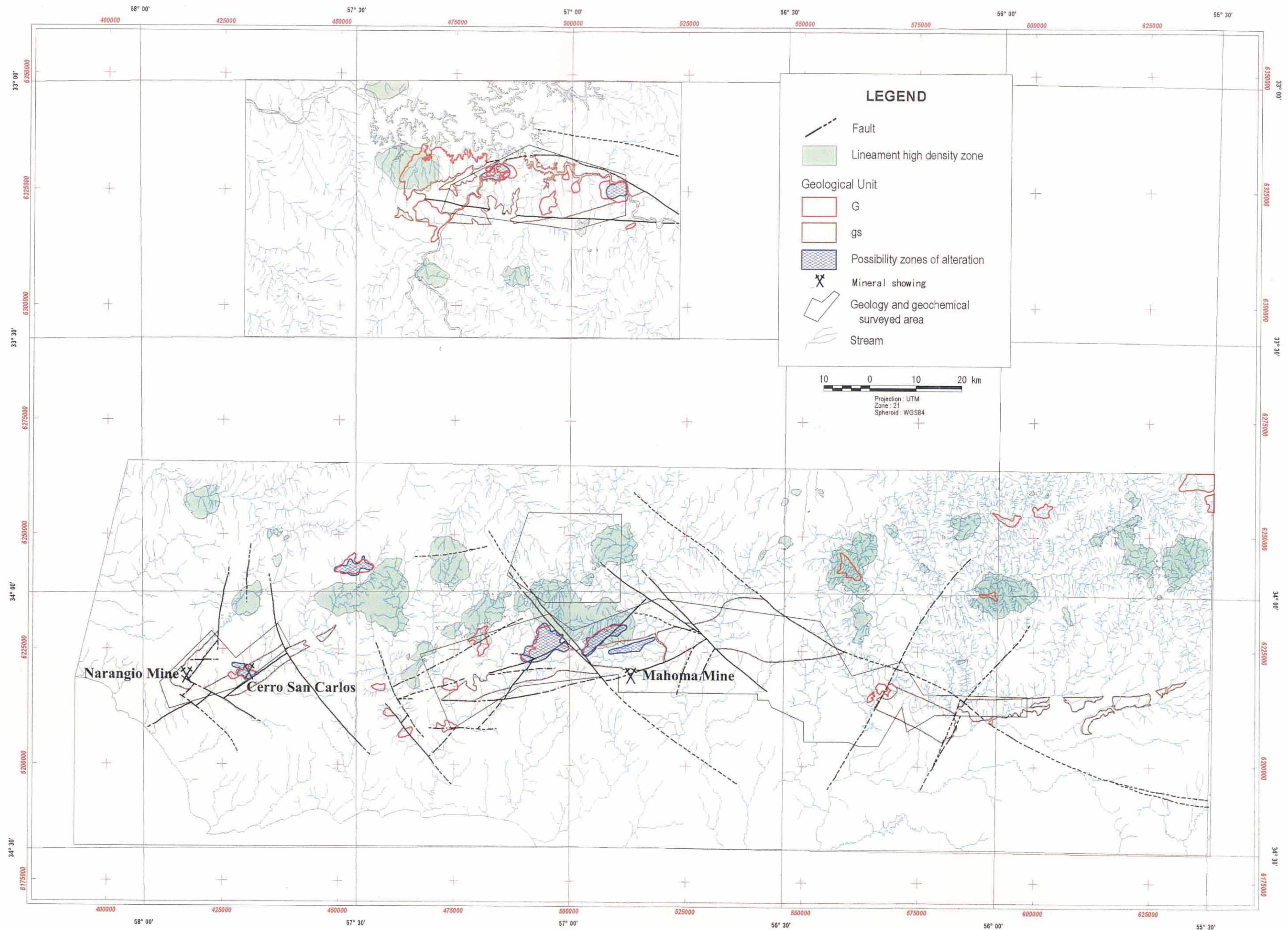


Fig. II -2-7 Interpretation map of satellite imagery

Tab.II-2-1 Image data used

JERS-1/SAR Imagery

| Path-Row | Date | Processed Level | Spatial Resolution | Band used | Off-nadir Angle | Polarization | Projection |
|-----------|----------|-----------------|--------------------|-----------|-----------------|--------------|------------|
| P397-R356 | 10/01/95 | L2.1 | 18.0m | L-Band | 35° | HH | UTM |
| P396-R356 | 09/01/95 | L2.1 | 18.0m | L-Band | 35° | HH | UTM |
| P398-R357 | 18/09/96 | L2.1 | 18.0m | L-Band | 35° | HH | UTM |
| P397-R357 | 10/01/95 | L2.1 | 18.0m | L-Band | 35° | HH | UTM |
| P396-R357 | 09/01/95 | L2.1 | 18.0m | L-Band | 35° | HH | UTM |
| P395-R357 | 12/10/94 | L2.1 | 18.0m | L-Band | 35° | HH | UTM |
| P394-R357 | 28/08/94 | L2.1 | 18.0m | L-Band | 35° | HH | UTM |
| P393-R357 | 06/01/95 | L2.1 | 18.0m | L-Band | 35° | HH | UTM |
| P399-R358 | 18/09/96 | L2.1 | 18.0m | L-Band | 35° | HH | UTM |
| P398-R358 | 10/01/95 | L2.1 | 18.0m | L-Band | 35° | HH | UTM |
| P397-R358 | 09/01/95 | L2.1 | 18.0m | L-Band | 35° | HH | UTM |
| P396-R358 | 12/10/94 | L2.1 | 18.0m | L-Band | 35° | HH | UTM |
| P395-R358 | 28/08/94 | L2.1 | 18.0m | L-Band | 35° | HH | UTM |
| P394-R358 | 06/01/95 | L2.1 | 18.0m | L-Band | 35° | HH | UTM |

LANDSAT/ETM+ Imagery

| Path-Row | Date | Processed Level | Bands | Spatial Resolution | | | Projection |
|-----------|----------|-----------------|-----------------|--------------------|----------|----------|------------|
| P224-R083 | 22/09/99 | L1G | Band 1 to 7 & P | 30m(VNIR & SWIR) | 60m(TIR) | 15m(Pan) | UTM |
| P223-R083 | 15/09/99 | L1G | Band 1 to 7 & P | 30m(VNIR & SWIR) | 60m(TIR) | 15m(Pan) | UTM |
| P224-R084 | 22/09/99 | L1G | Band 1 to 7 & P | 30m(VNIR & SWIR) | 60m(TIR) | 15m(Pan) | UTM |
| P223-R084 | 15/09/99 | L1G | Band 1 to 7 & P | 30m(VNIR & SWIR) | 60m(TIR) | 15m(Pan) | UTM |

Tab.II-2-2 Image products

| Products | Image data used | Scene number | Band used | Scale for interpretation | Projection | Spheroid | Zone |
|-----------------------|-----------------|--------------|-------------------|--------------------------|------------|----------|------|
| Digital mosaic of SAR | JERS-1/SAR | 14 | L | 1:250,000 | UTM | WGS84 | 21 |
| Digital mosaic of TM | LAMDSAT/ETM+ | 4 | B:G:R=1:4:5 | 1:250,000 | UTM | WGS84 | 21 |
| TM band ratio | LAMDSAT/ETM+ | 4 | B:G:R=3/1:5/4:5/7 | 1:250,000 | UTM | WGS84 | 21 |
| Investigation areas | | | | | | | |
| - San Jose east area | | | | | | | |
| - San Jose west area | | | | | | | |
| - Arroyo Grande area | | | | | | | |

Tab.II-2-3 Geologic interpretation chart

LANDSAT/TM mosaic

| Geologic units | Color | Drainage | | Resistance | Texture | Bedding(layering) | Vegetation/Landuse | Remarks | Comparison |
|----------------|-----------|---------------|--------------|--------------|------------|-------------------|--------------------|--------------------|-------------|
| | | Pattern | Density | | | | | | |
| a | black | braided | low | very low | even | - | dense | | Q |
| Q | green/red | dendritic | low | low | even | none | strong use | terrace-like | Q1 |
| T-K | green/red | dendritic | low | low | even | poor | strong use | | Ksa |
| Kb | green/red | dendritic | high | intermediate | rough | poor | strong use | San Jose area | Klm |
| Ka | magenta | sub-parallel | high | intermediate | rough | poor | less | Arroyo Grande area | Ksm, Kla1 |
| gn2 | green/red | sub-dendritic | high | intermediate | smooth | commom | strong use | | pCCcb |
| sh | magenta | sub-dendritic | high | intermediate | rough | developed | strong use | | pCCApd |
| | gs | green/red | sub-parallel | high | high | lineated | strong use | | pCCp.s.-sj. |
| | g | magenta | parallel | very high | high | lineated | common use | very layered | pCCG |
| | gn1 | magenta | dendritic | very high | high | rough | developed | common use | pCCcb |
| G | purple | sub-dendritic | very high | very high | very rough | none | low use | intrusives | pCC γ |

Footnote : comparison with existing map "Carta Geologica" procuded by Ministerio de Industria y Energia (1980), in scale of 1:500,000.

JERS-1/SAR mosaic

| Geologic units | Tone | Drainage | | Resistance | Texture | Bedding(layering) | Vegetation/Landuse | Remarks | Comparison | |
|----------------|------------|---------------|--------------|--------------|------------|-------------------|--------------------|--------------------|--------------|------|
| | | Pattern | Density | | | | | | | |
| a | light grey | braided | low | very low | even | - | dense | | Q | |
| Q | grey | dendritic | low | low | even | none | strong use | terrace-like | Q1 | |
| T-K | grey/white | dendritic | low | low | even | poor | intense use | | Ksa | |
| Kb | grey | dendritic | high | intermediate | rough | poor | strong use | San Jose area | Klm | |
| Ka | dark grey | sub-parallel | high | intermediate | rough | poor | less | Arroyo Grande area | Ksm, Kla1 | |
| gn2 | grey | sub-dendritic | high | intermediate | smooth | commom | strong | | pCCcb | |
| sh | dark grey | sub-dendritic | high | intermediate | rough | commom | strong use | | pCCApd | |
| | gs | dark grey | sub-parallel | high | high | lineated | developed | strong use | pCCp.s.-sj. | |
| | g | grey | parallel | very high | high | lineated | very developed | common | very layered | pCCG |
| | gn1 | grey | dendritic | very high | high | rough | developed | common | pCCcb | |
| G | light grey | sub-dendritic | very high | very high | very rough | none | poor | intrusives | pCC γ | |

Footnote : comparison with existing map "Carta Geologica" procuded by Ministerio de Industria y Energia (1980), in scale of 1:500,000.

CHAPTER 3 GEOLOGICAL SURVEY

3-1 Coverage and Purpose

The geological survey was carried out on the three areas, i.e. the main part of the San Jose area, the western part of the San Jose area and the Arroyo Grande area, in order to grasp the geological features and structure of the project area. The survey area is shown in Fig. II-3-1.

The main part of the San Jose area is located around the provincial capital of San Jose de Mayo of San Jose Province, about 80km northwest of the Capital Montevideo. The western part of the San Jose area is located to the northeast of the provincial capital Colonia of Colonia province facing the La Plata River. The Arroyo Grande area is located in the south of Rio Negro province, about 200km northwest of the Capital Montevideo. The topography surrounding these areas, consists of pastures forming flat peneplains that spread out over the locations.

3-2 Methodology

For the geological survey, geological description, photography and rock sampling were performed covering the outcrops and floats in the survey area, and a geological sketch of an outcrop was also carried out as the occasion demanded. Especially at the mineral showings, the location was obtained by summary survey and the detailed geological sketch was also made. For the field survey, the magnified topographical map drawn on a scale of 1:50,000 and the aerial photograph on a scale of 1:40,000 were both carried by the teams for reference while working on site. A route map was prepared on the basis of the topographical map, marking up the location of outcrops, geological distribution, rock sampling points and, the strike and dip of the schistosity and veins. Rock samples were taken, keeping in mind that the samples sufficiently represent the typical rocks and the lithofacies of the survey area, as well as the mutual correlation. GPS was used to confirm the location of outcrops and floats, and the latitude and longitude were obtained.

3-3 Result of laboratory experiments and analyses

The laboratory experiments and analyses were conducted on the rock samples gathered on the geological field survey, in order to set up the analysis of the survey area. The implemented items of the laboratory experiments and analyses were cut and described the thin sections and polished sections, X-ray diffractive analysis, whole rock analysis, chemical analysis, fluid inclusions analysis (homogenization temperature + salinity), and radiometric dating (K-Ar dating). The description of the thin sections, results of the whole rock analysis and results of radiometric dating are shown in Tab. II-3-1, 2 and 3, respectively, while the results of other experiments and analysis are described below. The location of the rock sampling point is plotted on the geological map Plate II-3-1, 2, 3 and 4, along with the items of laboratory analyses experimented on the sample.

3-4 Result of geological survey

3-4-1 Stratigraphy

The geological formation of this area mainly consists of basement complex (pCCcb, pCCanf), greenstone (pCCsjo, pCCsj, pCCps and pCCag), and ancient granite intrusive rocks (pCCG) and younger granite intrusive rocks (pCC). Cretaceous, Neogene and Quaternary systems unconformably overlay them. The geological map and the schematic stratigraphic columns are shown in Fig. II-3-2, 3 and 4, respectively.

(1) Basement complex (pCCcb, pCCanf)

The basement complex is distributed in the western extremity and east part of the main part of the San Jose area, and to the north of the western part of the San Jose area and also along the southern edge of the Arroyo Grande area. The basement contacts the upper formations with the NW-SE fault boundary in the western part of the San Jose area, and with the E-W fault boundary in the Arroyo Grande area, respectively. The basement complex is mainly composed of gneiss, schists, quartzite, amphibolite and granites, and accompanied by migmatite and hornfels. Granites shows weak foliation attributed to metamorphism. Quartz schist, metasandstone and siliceous rocks are predominant in the western part of the San Jose area. Amphibolite (pCCanf) is indicated apart from other lithofacies in the geological map because its distribution range is relatively massed.

Based on the microscopic examination, the quartz schist (Sample No. AR022) shows porphyroclastic texture, where quartz is imbedded as relict mineral in the matrix which has a well developed schistosity and consists of quartz, biotite and muscovite. The epidote amphibolite (AR059) is composed of amphibolite, epidote, quartz and titanite, and imbeds prismatic to granular porphyroblasts of amphibolite. The granite (FR010) shows weak foliation, and imbeds phenocryst of quartz, potassium feldspar, plagioclase and biotite. The sample subjected to age dating (AR126: amphibolite) is composed of quartz, plagioclase, amphibolite and epidote, and shows weak schistosity. In rare cases, quartz occurs as a small relict accompanying plagioclase.

(2) Greenstone

The greenstone is composed of the San Jose formation (pCCsjo) subjected to a relatively high grade metamorphism, and such formations subjected to a weak metamorphism as the Paso Severino (pCCps), the Cerros de San Juan (pCCsj) and the Arroyo Grande (pCCag) formations.

In the main part of the San Jose area, the San Jose formation subjected to a relatively high grade metamorphism is distributed on the south part of the E-W fault boundary, while the Paso Severino formation subjected to a weak metamorphism on the north side. In the western part of the San Jose area, the Cerros de San Juan formation subjected to a weak metamorphism is distributed, which partially has a fault contact with the basement complex. In the Arroyo Grande area, the Arroyo Grande formation subjected to a weak to moderate metamorphism is widely distributed. The common lithofacies of these four formations which are constituent of greenstone, are schist rocks (greenschist, mica schist and quartz schist), metavolcanic rocks and metasedimentary rocks.

(i) San Jose formation

The San Jose formation mainly consists of greenschist, mica schist, quartz schist, gneiss, metarhyolite, metabasalt, green rock, quartzite, metasandstone, slate, phyllite and amphibolite.

The quartz schist (DR034) shows porphyroclastic texture, where quartz and plagioclase are imbedded as relict mineral in the matrix, which has a developed schistosity and consists of plagioclase, muscovite and quartz. The amphibolite (CR006) is composed of quartz, plagioclase, epidote, amphibolite and actinolite, and in some cases quartz porphyroblast is imbedded. A weak preferred orientation in alignment of massive or tabular minerals is recognized. The green rock (BR029) is massive rock consisting of fine-grained epidote, titanite, chlorite, quartz, albite, carbonate minerals and magnetite. Considering the mineral assemblage, it is determined that the green rock is low grade metamorphic basic igneous rock.

(ii) Paso Severino formation

The Paso Severino formation consists of greenschist, mica schist, quartz schist, metabasalt, metagabbro, metasandstone, slate, phyllite and amphibolite.

The greenschist (AR026) is composed of such mineral assemblage characteristic of greenschist facies as quartz, albite, chlorite, actinolite and epidote but preferred mineral orientation is not recognized. The quartz schist (ER003) consists of fine-grained minerals of quartz, plagioclase, calcite, chlorite and muscovite, and shows a massive structure. The metabasalt (BR039) is recrystallized with a new metamorphic mineral assemblage of albite, actinolite, chlorite and epidote, although the former basalt porphyritic structure with phenocryst of peridotite is relict. The metagabbro (CR010) is completely replaced with a metamorphic mineral assemblage of chlorite, calcite, epidote, titanite, prehnite and actinolite and, the major part of the former texture of original rock disappears. The amphibolite (CR018) consists of such metamorphic minerals as hornblende, quartz, plagioclase and magnetite. The original igneous texture are not preserved at all. A weak foliation attributed to the preferred orientation of hornblende is recognized.

(iii) Cerros de San Juan formation

The Cerros de San Juan formation consists of greenschist, mica schist, quartz schist, talc, dolomite, metabasalt, metagabbro, metasandstone, slate, phyllite, amphibolite and dolerite.

According to the microscopic examination of the dolerite (AR106), phenocryst of peridotite is imbedded in the matrix consisting of fine-grained plagioclase and augite. It includes such alteration minerals as serpentinite, chlorite, actinolite, talc and magnetite.

(iv) Arroyo Grande formation

The Arroyo Grande formation consists of greenschist, mica schist, quartz schist, gneiss, metabasalt, metagabbro, metasandstone, slate, phyllite and amphibolite.

The metasandstone (ER077) consists of such metamorphic minerals as quartz, plagioclase, potassium feldspar and muscovite. In rare cases, it shows porphyroclastic texture, where quartz and potassium

feldspar are imbedded as relict mineral in the matrix of fine-grained metamorphic minerals. A weak foliation is recognized.

(3) Cretaceous system (Ksa)

Cretaceous system overlays unconformably the lower layer in the Arroyo Grande area and mainly consists of siliceous rock, agate and fine-grained sandstone.

(4) Neogene system (Tr)

Neogene system is scattered in the eastern part of the main part of the San Jose area and the central part of the western part of the San Jose area and overlays the lower layer unconformably. It mainly consists of mudstone, fine-grained sandstone, conglomerate and breccia.

(5) Quaternary system (Q)

Quaternary system mainly consists of sand, gravel and clay.

3-4-2 Intrusive rocks

(1) Ancient granite intrusive rocks (pCCG)

Ancient granite intrusive rocks are distributed as stock intrusive rock in the west to middle east parts of the main part of the San Jose area, the western part of the San Jose area and the central to northern parts of the Arroyo Grande area. The lithofacies mainly consists of middle to coarse-grained equigranular or porphyritic biotite granite, muscovite granite, granodiorite, diorite and quartz diorite, and is subjected to metamorphism. Ancient granite intrusive rocks are strongly weathered over all and disseminated by limonite. Generally the appearance occurs as massive intrusive rock, while it is subjected to cataclasis near the faults. Particularly, near the E-W and NW-SE faults in the middle west part of the main part of the San Jose area, it is observed that the foliation subjected to mylonitization and concordant with the fault directions is well developed.

Based on the microscopic examination, the biotite granite (GR004) shows blastoporphyritic texture, where quartz, potassium feldspar, plagioclase and biotite are imbedded as phenocryst and, relict minerals of plagioclase and potassium feldspar are included. The muscovite granite (AR056) includes quartz, potassium feldspar, plagioclase, muscovite and slight biotite as phenocryst, where the quartz has a mosaic texture. The granodiorite (CR001) includes quartz, plagioclase, amphiborite and slight magnetite as phenocryst. Wavy extinction in quartz and a slight deformation of the crystal structure in phenocryst are recognized. The granite (BR012) taken from near the E-W fault in the western part of the San Jose area is subjected to mylonitization. Such relict minerals as potassium feldspar, plagioclase, biotite and magnetite are recognized in the matrix of recrystallized fine-grained quartz. Most of the ancient granite intrusive rocks include such alteration minerals as muscovite, chlorite, epidote and carbonate minerals.

The sample subjected to age dating (BR001: biotite granite) is composed of quartz, potassium feldspar,

plagioclase, biotite, slight muscovite, apatite, magnetite and ilmenite, accompanying such alteration minerals as muscovite, chlorite, epidote, carbonate minerals and titanite. It is subjected to mylonitization and phenocryst of potassium feldspar and plagioclase is included in the matrix of recrystallized fine-grained quartz.

(2) Younger granite intrusive rocks (pCC)

Younger granitic rocks are scattered in the whole survey area of the main part of the San Jose area, the western part of the San Jose area and the Arroyo Grande area as stock intrusive rock. The lithofacies mainly consist of middle to coarse-grained equigranular or porphyritic biotite granite, muscovite granite, two mica granite, hornblende granite, leucogranite, granodiorite, diorite and tonalite, and partially accompanies aplite. It is rather heterogeneous when compared with the ancient granite intrusive rocks. Younger granite intrusive rocks usually form hillocks that are scores of meters higher than the surrounding flat topographic features, and the outcrop is in better condition than the surrounding area. Generally the appearance occurs as massive intrusive rock, and in some cases the foliation is developed being subjected to mylonitization. Based on the microscopic examination, the younger granite intrusive rocks include mainly quartz, potassium feldspar and plagioclase as phenocryst, such mafic minerals as biotite and muscovite or hornblende and biotite, and minor constituents of apatite, zircon, titanite and magnetite.

The features obtained by the microscopic examination on the samples subjected to the age dating process are as follows. AR125 (two mica granite) is mainly composed of quartz, potassium feldspar, plagioclase, muscovite and biotite, accompanying a trace of garnet and ilmenite. It is subjected to carbonitization and limonitization. It shows porphyroclastic fabric by mylonitization, where relict minerals of quartz, potassium feldspar and plagioclase are included.

AR128 (muscovite granite) is mainly composed of quartz, potassium feldspar, plagioclase and muscovite, with an accompanying trace of magnetite. It is subjected to chloritization and limonitization. It shows porphyroclastic texture by mylonitization, where relict minerals of quartz, potassium feldspar, plagioclase and muscovite are included. Grain size of the recrystallized quartz suggests multiple stage of shearing and recrystallization. AR129 (biotite granite) is mainly composed of quartz, potassium feldspar, plagioclase and biotite, accompanying a trace of zircon, apatite and magnetite. It is subjected to chloritization and limonitization. AR127 (leucogranite) is mainly composed of quartz, potassium feldspar and plagioclase, accompanying metamorphic mineral of muscovite.

(3) Intrusive rock : dolerite (dd)

Dolerite is distributed as a NE-SW dike in the central part and western edge of the main part of the San Jose area and intrudes principally in younger granite intrusive rocks (pCC). It is characterized by green massive lithologic character. Based on the microscopic examination, dolerite (CR048) shows massive epidote amphibolite facies composed of such metamorphic minerals as hornblende, plagioclase, epidote and magnetite.

(4) Intrusive rock : gabbro (gb)

Gabbro intrudes in the San Jose and Paso Severino formations mainly in the middle west part of the main part of the San Jose area, and crops out as stock. The lithologic character is dark-green gray hard dense rock facies. Based on the microscopic examination, gabbro (BR006 and BR015) is mainly composed of peridotite, augite, plagioclase and magnetite and includes such metamorphic minerals as talc, chlorite, epidote, carbonate minerals and serpentinite.

(5) Chemical composition

The Total alkalis ($\text{Na}_2\text{O}+\text{K}_2\text{O}$) vs Silica (SiO_2) diagram (TAS) and the Harker variation diagrams for granitic intrusive rocks (pCCG and pCC) are shown in Fig. II-3-5 and 6, respectively. The SiO_2 contents of the granitic intrusive rocks is within a range of about 47~78wt.%. Based on the TAS diagram, most of the samples are classified as subalkalic series, and plotted on the fields of granite, granodiorite, diorite and gabbro. Based on the Harker variation diagrams, the samples that contain more than 60% SiO_2 show negative correlations of SiO_2 vs TiO_2 , Al_2O_3 , Fe_2O_3 , MnO, MgO and CaO. In contrast, the samples that contain lower than 60% SiO_2 are scattered on the diagrams, and clear trends are unrecognized. Positive correlation is observed for the K_2O vs SiO_2 diagram.

(6) Radiometric age

Ancient granite intrusive rocks (pCCG) were dated from the biotite granite (BR001) corresponding to the host rock of the Mahoma mine in the middle west part of the main part of the San Jose area, and the age was obtained as $1960 \pm 140\text{Ma}$ by K-Ar method. This age is significantly young, when compared with the age before 2200Ma described in the existing information. It is considered that the ancient granite intrusive rocks are under the influence of rejuvenation, due to recrystallization by mylonitization as well as mineralization and alteration of the Mahoma mine.

Younger granite intrusive rocks (pCC) were dated from different samples. The age was indicated $1690 \pm 120\text{Ma}$ from the two mica granite (AR125) of the western part of the San Jose area, while $1240 \pm 10\text{Ma}$ and $1750 \pm 120\text{Ma}$ from the muscovite granite (AR128 : Mal abrigo granite) and the biotite granite (AR129 : Mahoma granite) respectively, both of which are distributed in the middle west part of the main part of the San Jose area. It was indicated $1980 \pm 130\text{Ma}$ from the leucogranite (AR127) of the Arroyo Grande area. Based on the existing information, younger granite intrusive rocks (pCC) were formed in about 1800 to 2000Ma and correlated with the igneous activity in the Transamazonian orogenesis.

The age obtained from the two mica granite (AR125) of the western part of the San Jose area, the biotite granite (AR129) of the main part of the San Jose area and the leucogranite (AR127) of the Arroyo Grande area, are consistent with the age described in the existing information, within the error range. The younger indicated age of muscovite granite (AR128) of the main part of the San Jose area is subjected to a strong mylonitization, based on the microscopic examination. Consequently it is considered that the younger age is under the influence of rejuvenation due to recrystallization.

As for the amphibolite (AR126) of the east part of the main part of the San Jose area, the age was obtained as 2000 ± 280 Ma. This rock is set down as the basement complex rocks in the geological map on a scale of 1:500,000 within the existing information, while it has been set down as younger intrusive rocks by the JMEC (2001).

3-4-3 Metamorphism

All of the San Jose (pCCsjo), the Paso Severino (pCCps), the Cerros de San Juan (pCCsj) and the Arroyo Grande (pCCag) formations which are constituent of greenstone, are subjected to metamorphism, and the lithologic facies are mainly metasedimentary rocks and metavolcanic rocks. Based on the result of the microscopic examination, the metasedimentary rocks consist of muscovite quartz rock and pelitic schist, and includes such metamorphic minerals as quartz, plagioclase, muscovite, carbonate minerals, apatite, titanite, limonite and opaque minerals.

The original rock of the metavolcanic rocks varies from acidic to basic rocks. However, basic metamorphic rocks such as metabasalt and metagabbro are predominant in the survey area, except the Arroyo Grande area. The basic metamorphic rocks show metamorphic facies mainly as greenschist facies, epidote amphibolite facies and amphibolite facies. The greenschist (AR026, BR029, BR039 and GR017) is characterized by the mineral assemblage of actinolite, chlorite and epidote, accompanying quartz, albite, carbonate minerals, titanite and limonite. The epidote amphibolite (AR033 and CR009) is characterized by the mineral assemblage of albite, hornblende and epidote. The amphibolite (CR018) consists of hornblende, plagioclase and quartz as its main mineral component, and does not include chlorite and epidote. The greenstone of the survey area, which shows such metamorphic facies composed of the above-mentioned greenschist, epidote amphibolite and amphibolite, is determined to be formed by metamorphism under a low- to middle-grade pressure.

3-4-4 Geological structure

The geological structure of the survey area is characterized by the faults general trends of E-W and NW-SE. The E-W fault forms the boundary between the San Jose formation on the south side and the Paso Severino formation on the north side, in the south part of the main part of the San Jose area. In the central part of the main part of the San Jose area, the boundary between the San Jose formation and the Paso Severino formation concordant with the E-W fault, is observed in parallel. The schistosity direction of metamorphic rock is almost concordant with the E-W fault. In the Arroyo Grande area, the well continued E-W fault forms the boundary between the basement complex on the south side and the Arroyo Grande formation in the north.

The NW-SE fault controls the distribution of ancient granite intrusive rocks, basement complex and the Cerros de San Juan formation, in the western part of the San Jose area. In the middle west part of the main part of the San Jose area, the schistosity close to the fault is controlled in a NW-SE direction, and younger granite intrusive rocks (pCC) are strongly subjected to mylonitization. Displacement of fracture is not

recognized at each outcrop. However, considering the geological distribution of the surrounding area, it is determined that the NW-SE fracture has a right lateral slip component.

3-4-5 Ore deposit

As the result of the field survey, the following 13 mineral showings were found as a zone where the quartz vein had been developed (Fig. II-3-7). Descriptions about each mineral showing are resumed in Tab. I-5-1.

The main part of the San Jose area (10 mineral showings)

- A: surrounding area of the Mahoma mine (20km EW × 15km NS)
- B: Nueva Helvecia (the western extremity of the area : 10km × 18km)
- C: Arroyo del Medio (6km × 15km)
- D: Canada de Cabrera (8km × 4km)
- E: Arroyo charruzo (10km × 12km)
- F: Tala I (3km × 4km)
- G: Tla II (9km × 14km)
- H: West of 25 de Mayo (6km × 8km)
- I: South of 25 de Mayo (10km × 10km)
- J: San Ramon (the eastern extremity of the area : 10km × 5km)

The western part of the San Jose area (1 mineral showing)

- K: San Carlos (21km × 13km)

The Arroyo Grande area (2 mineral showings)

- L: Rio Negro I (10km × 15km)
- M: Rio Negro II (25km × 10km)

The gold-bearing quartz vein is impregnated with the basement complex (pCCcb and pCCanf), ancient granite intrusive rocks (pCCG) and greenstone (pCCps, pCCsj, pCCag and pCCsjo).

Wall rock alteration : The wall rock alteration was analogized as follows, based on the observation result of restricted outcrops including the open cuts of the Mahoma mine, because the outcrops were poorly developed in the survey area. It is megascopically recognized that both granites and greenstone of the wall rock are subjected to silicification at the edge of the quartz vein. The silicification range is in proportion to the vein width, and the silicification area tends to cover a wider range, the wider the vein width is. Chloritization and epidotization are also recognized in most of greenrocks and some of granites. The result of X-ray diffractive analysis is shown in Tab. II-3-4. The mineral assemblages consisting of quartz – sericite – (pyrite) and chlorite – epidote – (albite), are estimated from the edge of the quartz vein outwards.

Occurring appearance of quartz veins : The vein width comes to several to dozens of meters in basement rocks, greenstone and ancient granitic rocks, while it declines extremely to several centimeters to millimeters in younger granite intrusive rocks (pCC). It is considered that pCC somehow contributed to the gold mineralization. In the wall rock around the pCC body, quartz veins are well developed.

However the geological information of pCC as directly associated igneous rocks, is not obtained. Assuming a series of ore-forming processes, the following causes are estimated as reasons for diminution of the quartz vein width in pCC.

The lithologic character of pCC is inhomogeneous, when compared with pCCG. Large fissures were not formed because creeping deformation occurred due to its high ductility. Conversely, fractures with a moderate width could not be formed because brittle deformation occurred due to its low ductility.

Disposition pattern of the quartz vein : Two preferred directions of the quartz veins are observed; the NE-SW to E-W and the NW-SE. The former is approximately concordant with the geological structure as typified by faults and schistosity plane. Based on existing information, there is a description about a large-scale fracture zone displaying left lateral slip as the predominant E-W trending geological structure in this survey area. Regarding the latter NW-SE direction, NW-SE quartz vein shows the echelon disposition, at the mineral showing M (Rio Negro II) in the Arroyo Grande area, and the disposition pattern is "left echelon". Consequently the NW-SE trending vein displays right lateral slip sense, and accompanies faults developed in the same sense in the main part of the San Jose area and the western part of the San Jose area. It is considered that the NW-SE faults, which are the most recent structure in this survey area, can be a conjugate set with the NE-SW to E-W veins.

Mineralization : Based on the result of the polished section observation for both samples of quartz vein and wall rock, ore mineral was hardly found in the quartz vein except a little limonite and partially an infinitesimal amount of pyrite (Tab. II-3-5). A small amount of pyrite – (chalcopyrite) dissemination was recognized in green rocks and some part of the quartz vein. Based on the assay result, as described in Chapter 5, the maximum assay value was 19,890ppb (Appendix 4).

From the lithologic character of the quartz vein, it was classified into three types, milky sugar-like translucent quartz, colorless to white transparent quartz and gun metal transparent quartz. Considering the zonal distribution, which is locally recognized, and their appearance of interpenetration, it is estimated that these different stages of each quartz type become recent in this order in a chronological relationship. However it is difficult to determine each mineralization stage because the outcrop condition was generally bad and these types of quartz occurred together.

2, 1, 5, 4 and 2 samples were taken from the mineral showing A, C, E, G and M respectively, in order to subject them to the fluid inclusion analysis. As a result, the homogenization temperature was estimated to be 447.7°C at the highest and 85.6°C at the lowest, and the histogram usually had three peaks at around 300°C, 250°C and 200 to 150°C, which could be considered to correspond to milky translucent quartz, colorless to white transparent quartz and gun metal transparent quartz, respectively. Based on the result of measurement, the salinity was 4.2 to 35% (NaCl % equivalent), which indicates a coexistence of both quartz formed under high and low pressure.

Considering which type of quartz is accompanied by Au, no characteristic depending on the mineral showing is recognized. It seems that Au is apt to accompany colorless to white transparent quartz and gun metal transparent quartz. In addition to these types, black quartz also occurs which contains clay minerals

(phyllosilicate) difficult to identify. Consequently it is necessary to carefully analyze in more detail to be able to discuss the ore-forming stage of quartz accompanied by Au.

Next regarding the representative Mahoma mine in the survey area. The Mahoma mine is located in and belongs to the mineral showing A, slightly west of the center of the main part of the San Jose area, about 30km northwest of San Jose, a 35 minute drive. According to existing information, the prospecting was carried out from 1986 to 1990, and the digging was worked from 1992 to 1995. 2~3 kg of gold was produced. The wall rock is chloritized diorite to granodiorite.

Among the three open cuts remaining now, the western side of one of the outcrops, can be observed. The detailed ore deposit survey was implemented on this. The open cut is about 350m long in an EW direction, about 30 to 50m wide in the NS direction and about 10m deep, and the deeper part is now submerged. At that time, it was described as a trench dug 100m in length.

As shown in the Fig. II-3-9, the white transparent quartz vein 15 to 70cm wide and the reddish-blown limonite – quartz vein 2 to 5cm wide are recognized, showing the strike of 80° E and the dip of 87° N. According to existing information, only limonite is recognized as ore mineral, while there are descriptions about native gold of 20 to 40 μ m occurring interstitially at a spot in the quartz grains in the quartz vein, and native gold of 1520 to 40 μ m occurring in pyrite.

Based on the assay result, the assay values were Au: 1,520ppb for the sample of vein quartz, and Au: 291 to 111ppb for the wall rock sample. The assay value declines with the distance from the vein. Based on the result of X-ray diffractive analysis, it was found that sericite is included in the limonite – quartz vein.

At the east part of the mineral showing K in the western part of the San Jose area, a dump remains of the Cerro San Carlos mine vestige is found in a distribution area of granites (pCCG), although the details are unknown. Based on the assay result, the assay values were Au: 1,548ppb for the float of quartz vein, and Au: 115ppb for the float of wall rock.

The working Naranjio talc mine is located in the west part of the same mineral showing K. This mine was opened in 1904 for open-pit mining and from 1972 onward the mining method was changed to underground mining. Now the digging goes down approximate 70m below ground and the monthly production is 50 tons. It is said that the white part is used for ceramics and the green part for pigment.

This is a vein ore deposit, having a strike of N10° E to N45° E and a dip of 80° E to 85° NW. The wall rock is white dolomite (which does not appear on the surface) borne in the dark gray mafic rocks included in the greenstone (pCCsj). The vein width is 2 to 20m.

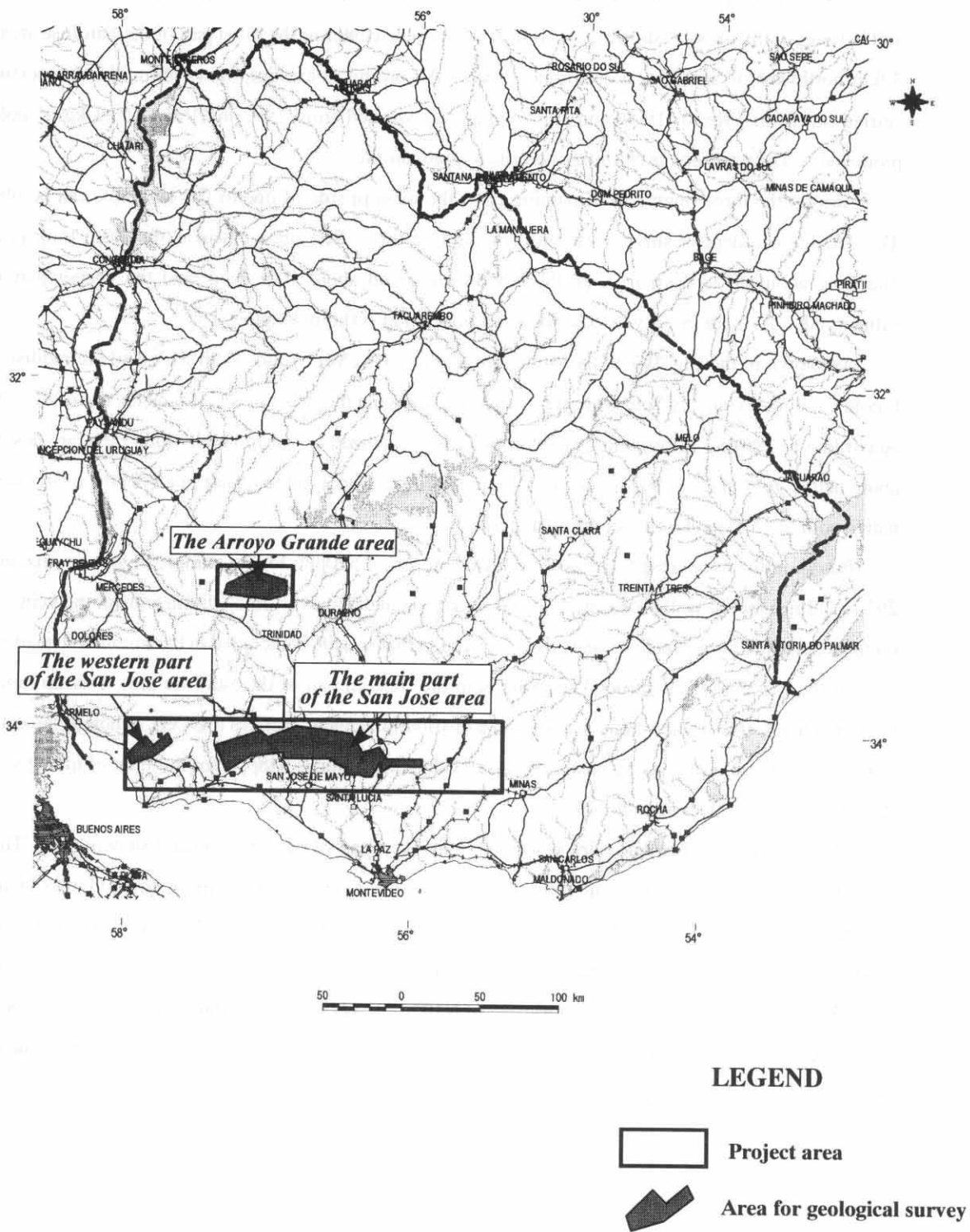
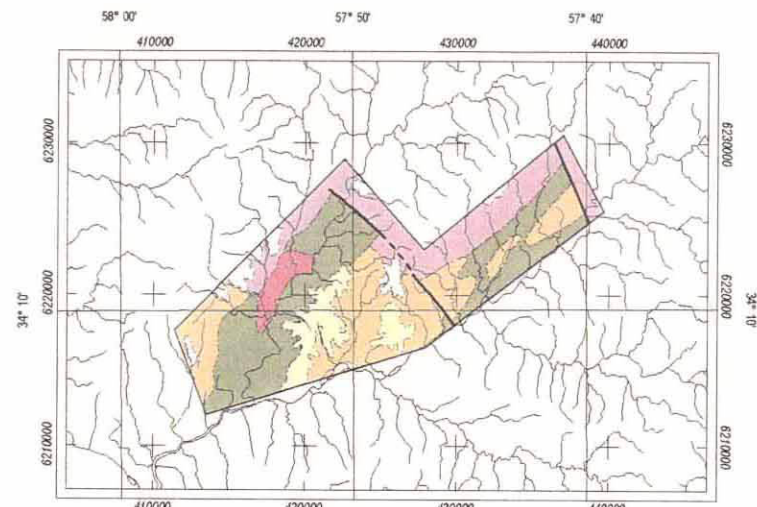
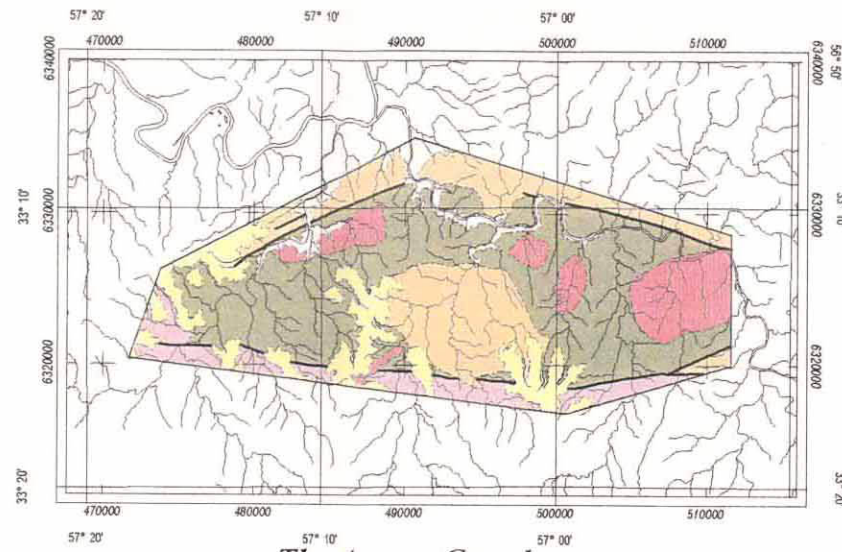


Fig.II-3-1 Location of the area for geological survey



The western part of the San Jose area



The Arroyo Grande area

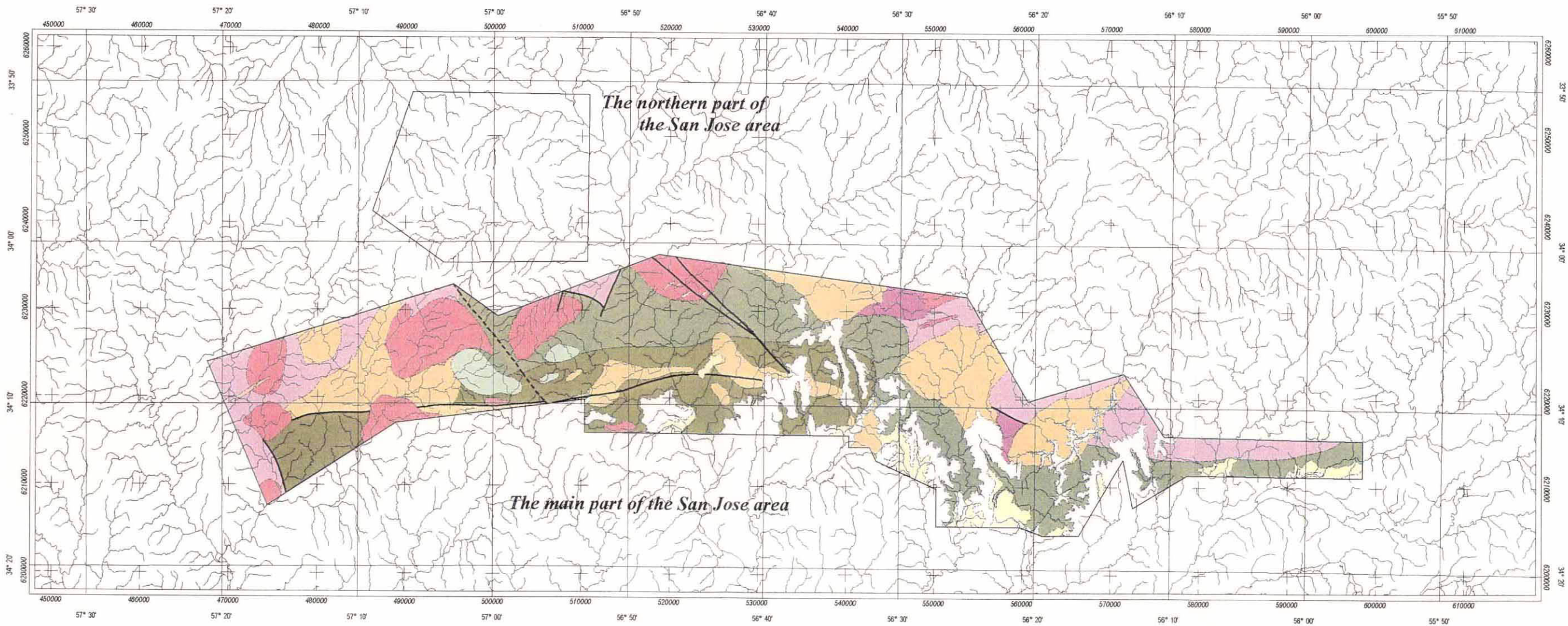
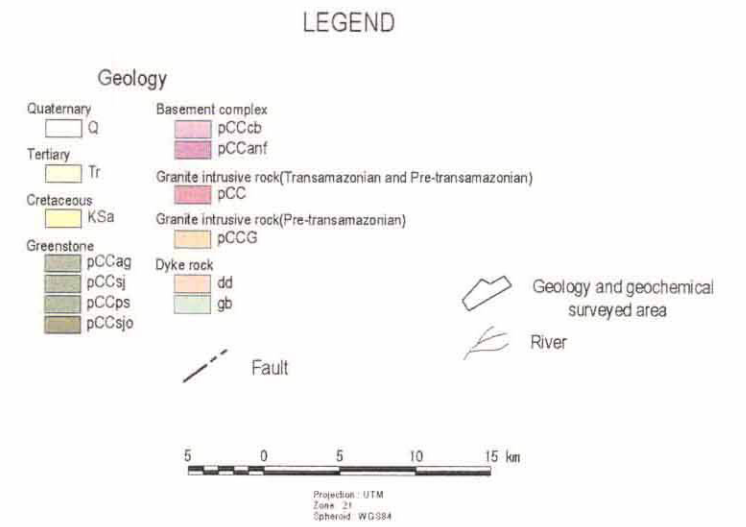


Fig.II-3-2 Geological map

| AGE (Ma) | | UNITS | EVENTS | DOMAIN |
|--------------|--|---|---|------------------------------|
| 1400? - 1800 | <i>pCC</i> (<i>pECy</i>)* | Doleritic dykes | Distensive enviroments | TRANSAMAZONIAN OROGENESIS |
| | | | CRATONIZATION | |
| 1894 - 1925 | | Pintos granite (1845 Ma) Aplites and granitic dykes of A° de la Virgen | | |
| 2000 | | Mahoma granite (1930 Ma) Conchillas granite (1970 Ma) Granite - Gneissic Complex Minuano granite (2000 Ma) Carmelo granite (2015 Ma) Florida granite (2030 Ma) | | |
| 2040 | | Granitic dyke of Isla Mala Gabbroic Complex Mahoma - Guaycurú | | |
| 2070 - 2100 | | | Metamorphism migmatization, granititation and folding | |
| 2225 | | A° de la Virgen leucogranite | Late - orogenic | PRE TRANSAMAZONIAN |
| | | | MILONITIZATION | |
| 2290 | | Isla Mala leucogranite | | |
| 2450 | | Isla Mala Granodiorite | | |
| 2500 | <i>pCCps</i> (<i>pECps</i>)* <i>pCCsjo</i> (<i>pECsjo</i>)* | San José metamorphism belt with first big deformation phase older than 2500 Ma | | ARCHEAN |
| ? | <i>pCCcb</i> (<i>pECps</i>)* | Complejo Basal | | |

* nomenclature used in the Carta Geológica del Uruguay. Escala 1:500,000 (1985)

Modified from Preciozzi, F.(1999). Petrography and Geochemistry of five Granitic Plutons from South - Central Uruguay: Contribution to the knowledge of the Piedra alta Terrane. Thesis, Universidad Quebec - Canadá.

Fig.II-3-3 Schematic stratigraphic column of the San Jose are

| AGE (Ma) | | UNITS | EVENTS | DOMAIN |
|-------------|---------------------------------|--|--|-------------------------------------|
| 1969 | <i>pCC</i> <i>(pECy)*</i> | Leucogranite dykes | | <i>TRANSAMAZONIAN</i> |
| 2067 | | Leucogranite | III Deformational phase | |
| 2180 | | South Granite | Contemporaneous with Paso del Lugo Fault | <i>PRE</i> <i>TRANSAMAZONIAN</i> |
| 2275 - 2386 | | Marincho main Granodiorite | II Deformational Phase | |
| 2501 - 2557 | <i>pCCag</i> <i>(pECag)*</i> | Alkaline - Granite Blocks Arroyo Grande Belt Metamorphic Rocks | I Deformation Phase | <i>ARCHEAN</i> |

* nomenclature used in the Carta Geológica del Uruguay. Escala 1:500,000 (1985)
 Modified from Preciozzi, F. (1999). Petrography and Geochemistry of five Granitic Plutons from South - Central Uruguay: Contribution to the knowledge of the Piedra alta Terrane. Thesis, Universidad Quebec - Canadá.

Fig.II-3-4 Schematic stratigraphic column of the Arroyo Grande are

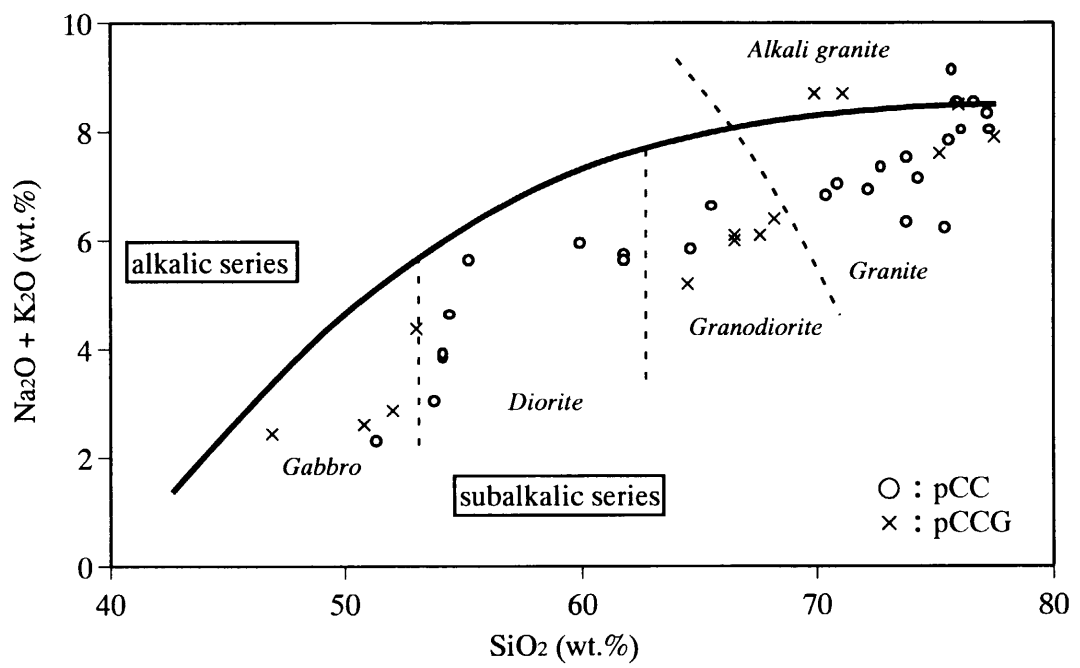


Fig.II-3-5 TAS diagram for granitic rocks

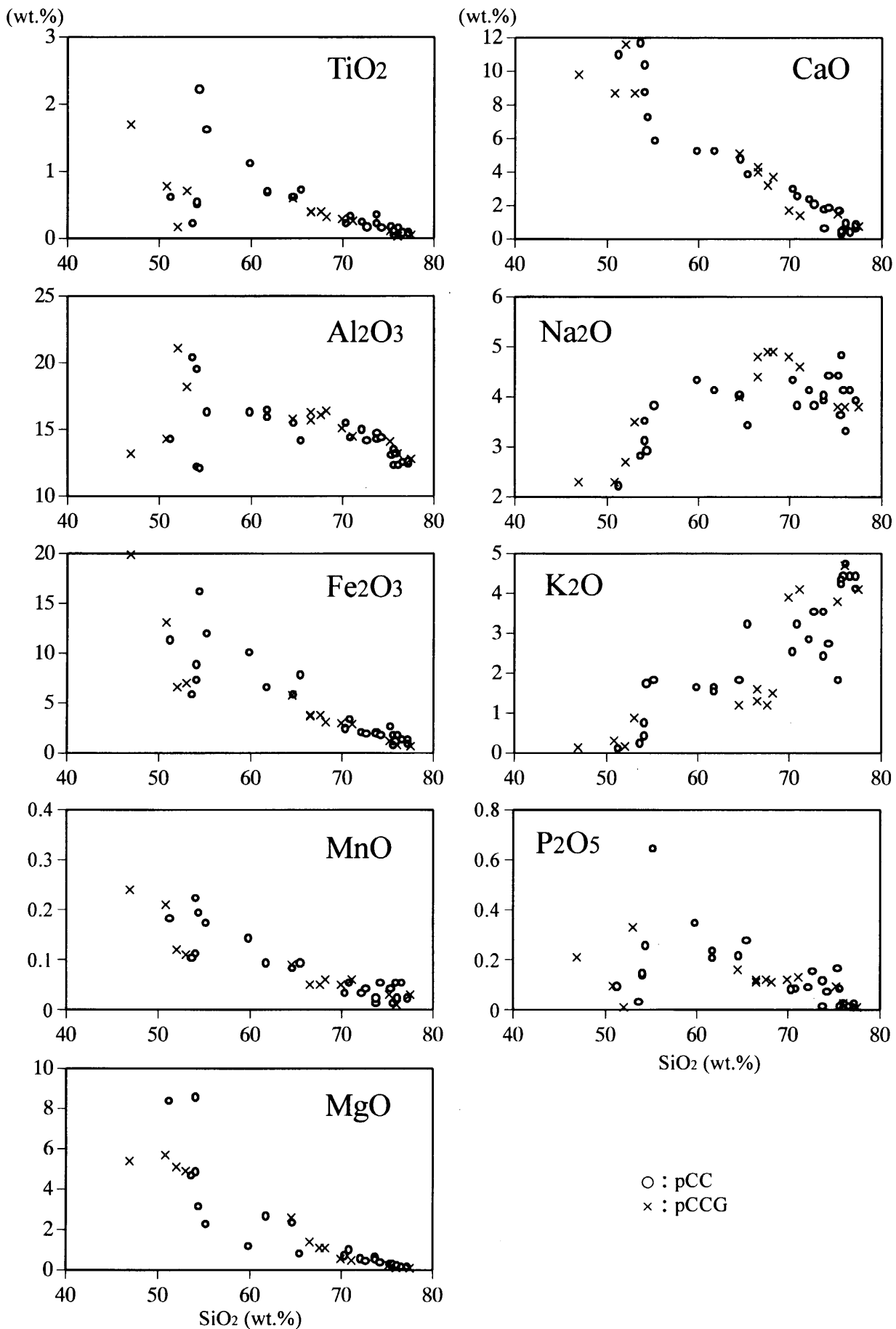


Fig.II-3-6 Harker variation diagrams for granitic rocks

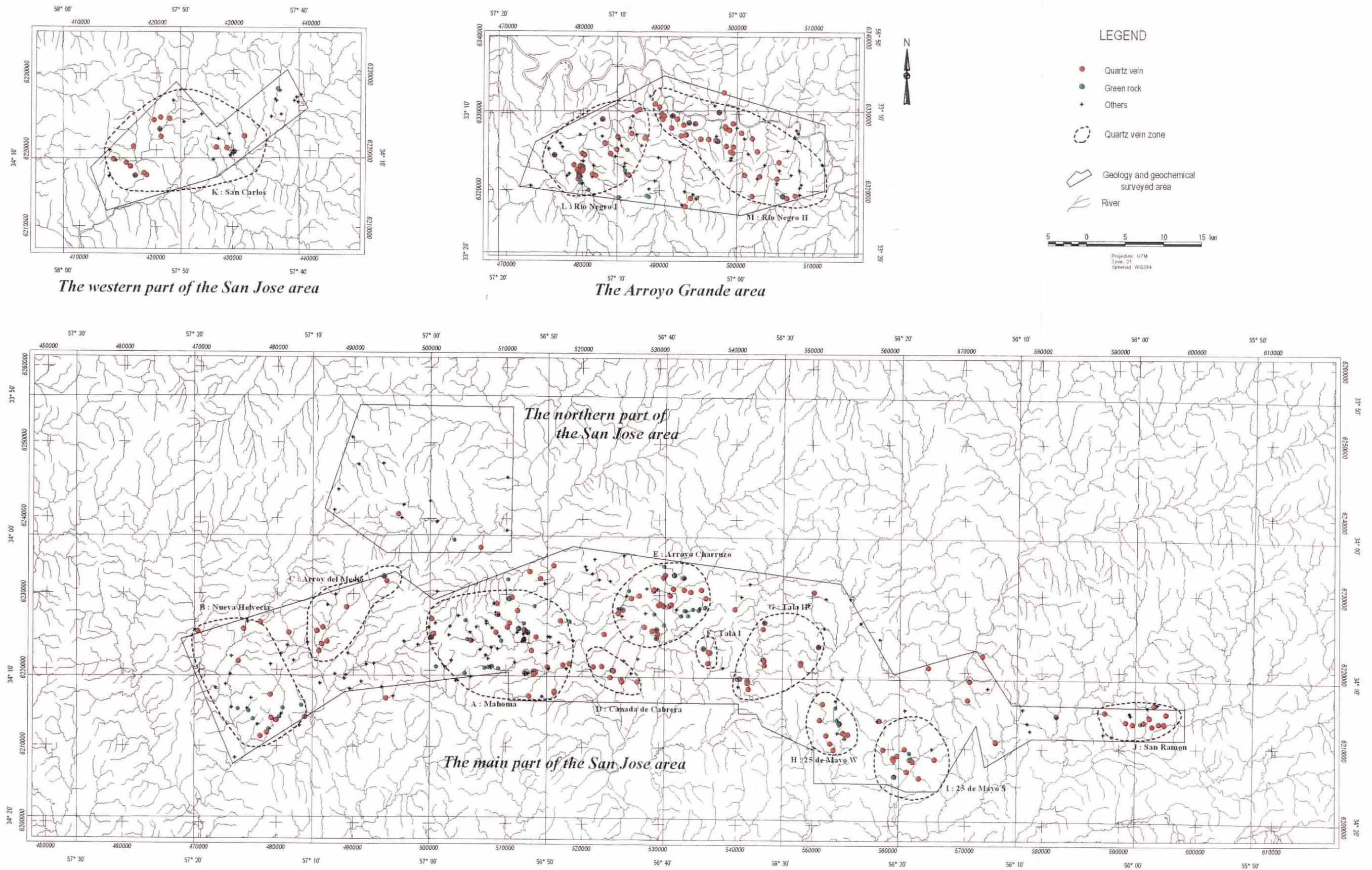


Fig.II-3-7 Location map of the quartz vein zones with location of geochemical rock samples

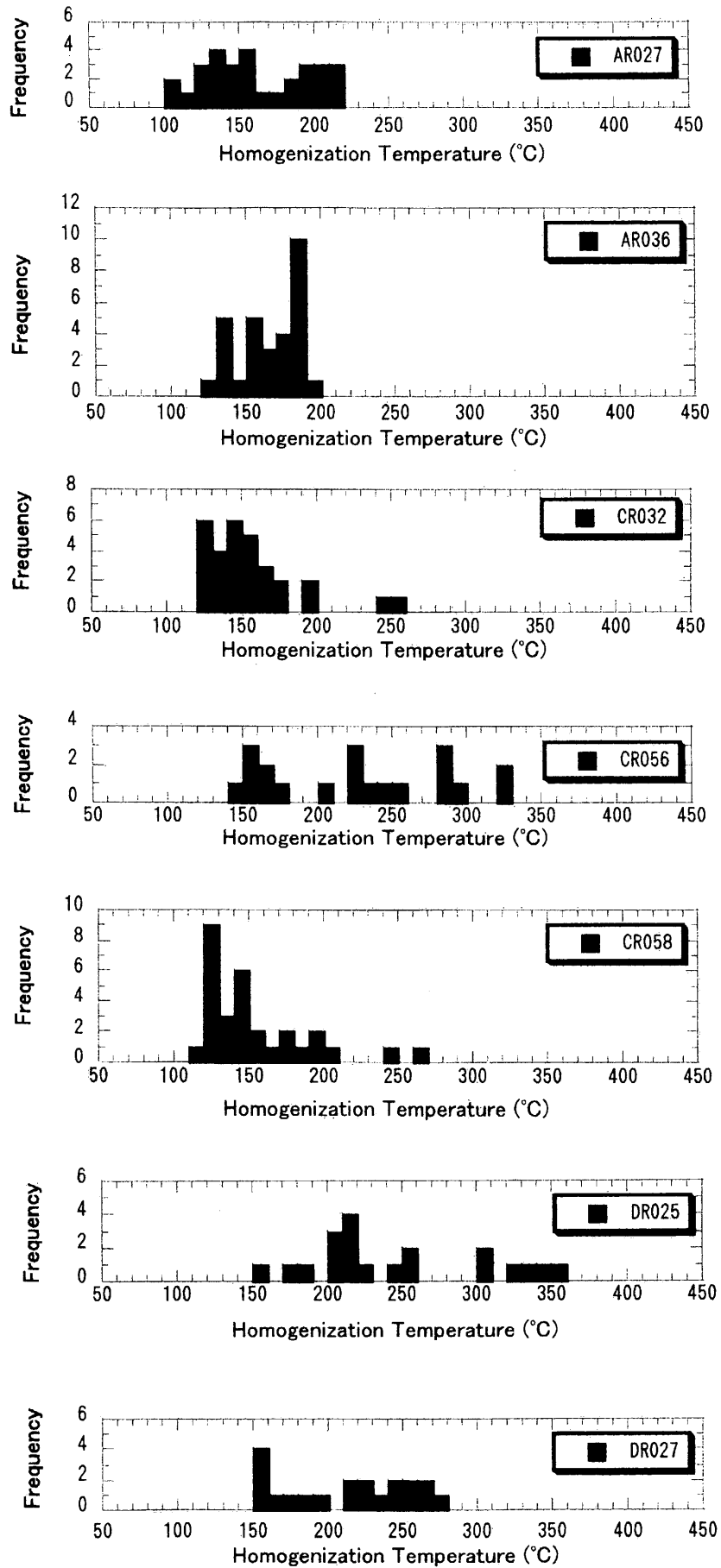


Fig.II-3-8 Histogram of fluid inclusions of quartz veins (1)

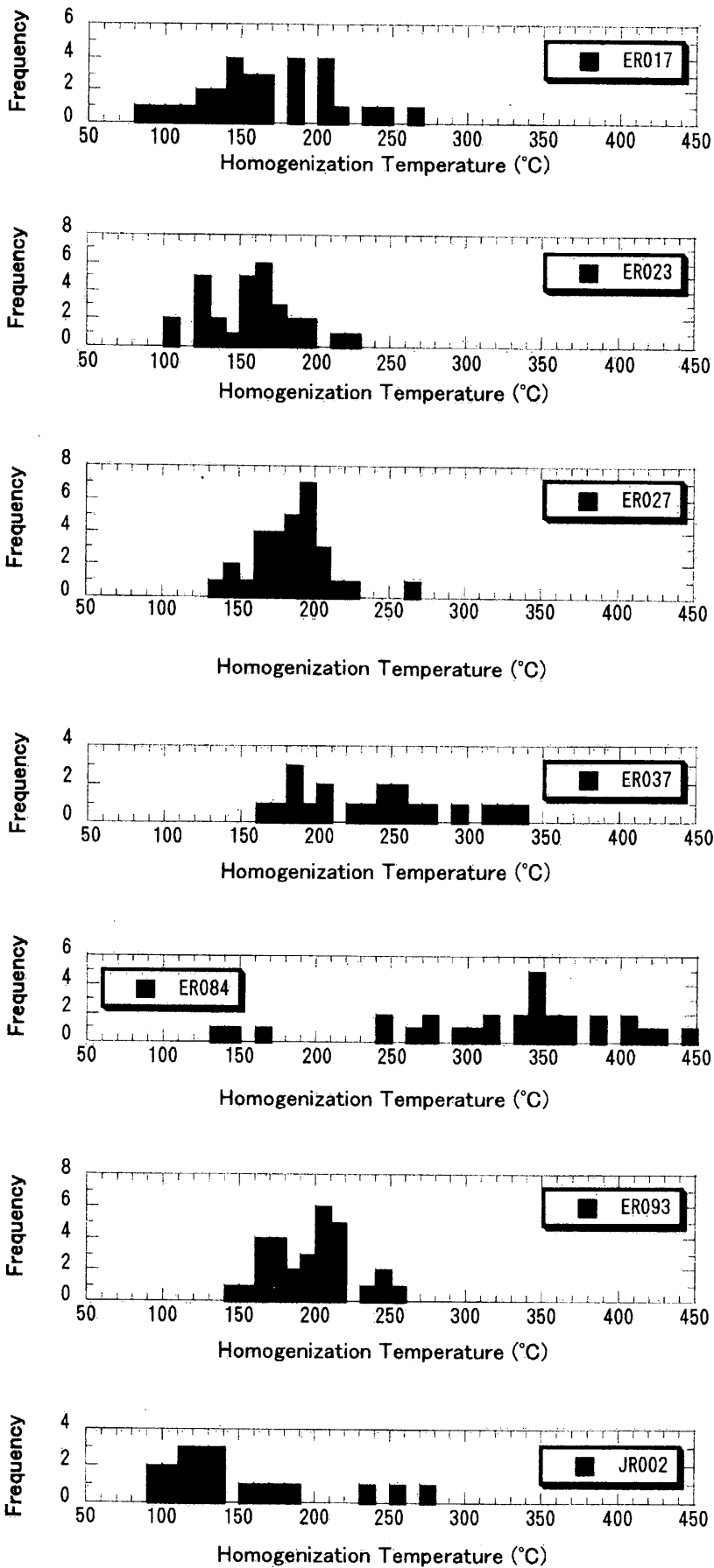
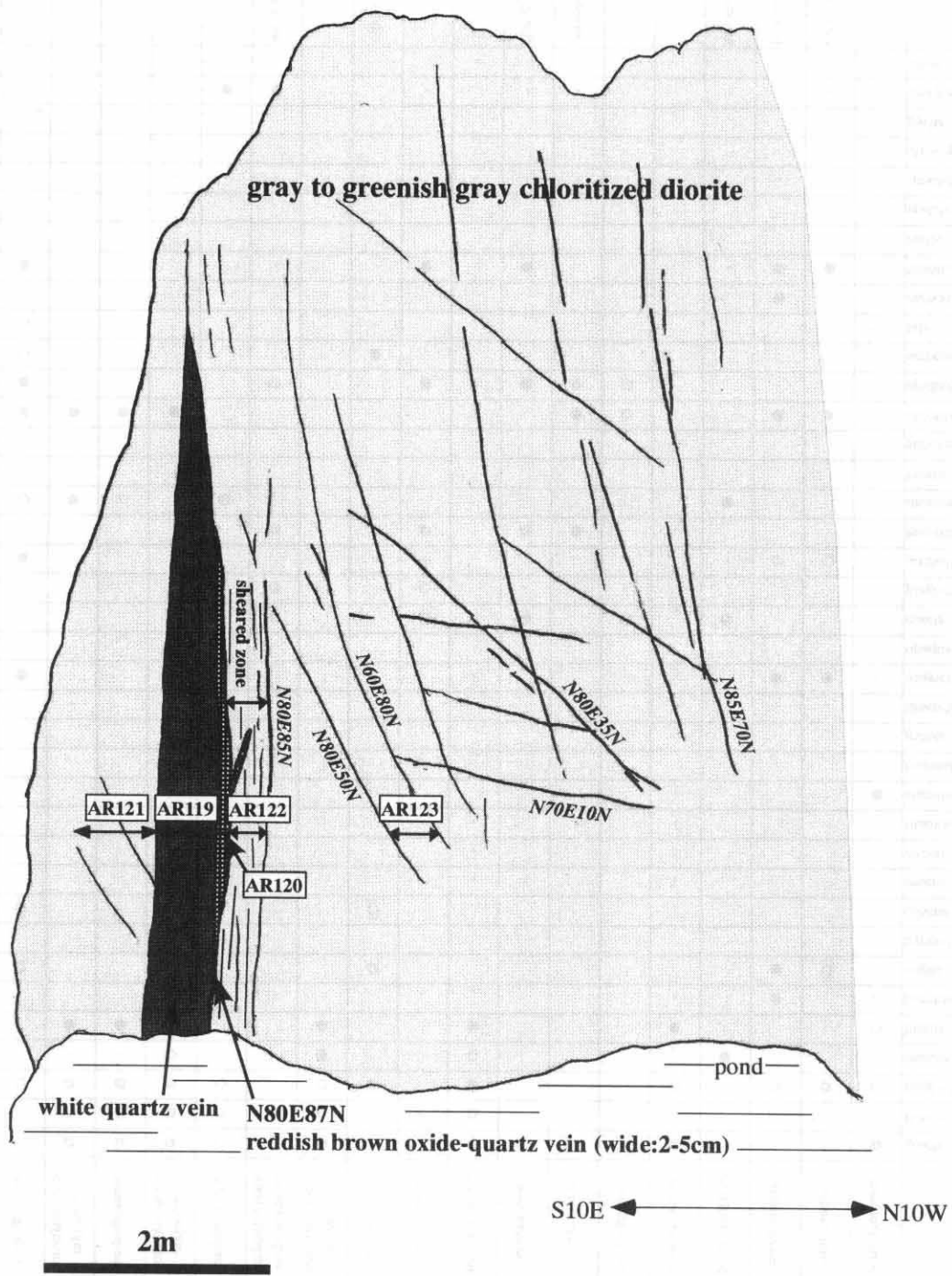


Fig.II-3-8 Histogram of fluid inclusions of quartz veins (2)



| Sample No. | Au (ppb) |
|------------|----------|
| AR119 | 1520 |
| AR120 | 1550 |
| AR121 | 143 |
| AR122 | 291 |
| AR123 | 111 |

Fig.II-3-9 Geological sketch of quartz vein of the Mahoma mine

Tab. II -3-2 Results of whole rock analysis (1)

| Ser. No. | Sample No. | Area | Rock Name | Geol.Unit | SiO ₂ | TiO ₂ | Al ₂ O ₃ | Fe ₂ O ₃ | MnO | MgO | CaO | Na ₂ O | K ₂ O | Ci ₂ O ₃ | P ₂ O ₅ | LOI | Total |
|----------|------------|------|---------------------|-----------|------------------|------------------|--------------------------------|--------------------------------|------|--------|-------|-------------------|------------------|--------------------------------|-------------------------------|------|--------|
| 1 | AR014 | MSJ | diorite | gb | 65.40 | 0.36 | 16.80 | 3.80 | 0.05 | 1.50 | 4.70 | 4.50 | 1.40 | < 0.01 | 0.130 | 0.78 | 99.42 |
| 2 | AR019 | MSJ | diorite | pCCG | 46.90 | 1.70 | 13.20 | 19.90 | 0.24 | 5.40 | 9.80 | 2.30 | 0.14 | < 0.01 | 0.210 | 0.26 | 100.05 |
| 3 | AR026 | MSJ | green schist | pCCps | 53.80 | 1.30 | 16.00 | 11.60 | 0.17 | 5.30 | 5.50 | 3.60 | 0.03 | 0.02 | 0.400 | 3.17 | 100.89 |
| 4 | AR033 | MSJ | amphibolite | pCCps | 49.20 | 0.94 | 14.00 | 13.20 | 0.19 | 6.90 | 11.40 | 1.80 | 0.10 | 0.03 | 0.083 | 2.36 | 100.20 |
| 5 | AR042 | MSJ | granodiorite | pCC | 75.50 | 0.15 | 13.00 | 2.50 | 0.04 | 0.22 | 1.60 | 4.40 | 1.80 | < 0.01 | 0.160 | 0.87 | 100.24 |
| 6 | AR043 | MSJ | amphibolite | dd | 61.50 | 0.82 | 10.30 | 11.80 | 0.11 | 3.20 | 11.30 | 0.46 | 0.04 | 0.05 | 0.310 | 0.37 | 100.26 |
| 7 | AR045 | MSJ | granodiorite | pCC | 61.90 | 0.66 | 15.80 | 6.40 | 0.09 | 2.60 | 5.20 | 4.10 | 1.60 | 0.03 | 0.230 | 0.61 | 99.22 |
| 8 | AR055 | MSJ | leucocratic granite | pCCG | 77.50 | 0.05 | 12.80 | 0.69 | 0.03 | < 0.10 | 0.75 | 3.80 | 4.10 | < 0.01 | < 0.010 | 0.22 | 99.94 |
| 9 | AR056 | MSJ | leucocratic granite | pCCG | 76.00 | 0.03 | 13.20 | 0.81 | 0.01 | 0.11 | 0.47 | 3.80 | 4.70 | < 0.01 | 0.026 | 0.36 | 99.52 |
| 10 | AR059 | MSJ | amphibolite | pCCcb | 48.90 | 0.78 | 16.20 | 12.40 | 0.21 | 5.50 | 13.60 | 1.50 | 0.12 | 0.01 | 0.094 | 0.45 | 99.76 |
| 11 | AR080 | AG | granodiorite | pCC | 65.60 | 0.71 | 14.10 | 7.70 | 0.09 | 0.76 | 3.80 | 3.40 | 3.20 | 0.03 | 0.270 | 0.37 | 100.03 |
| 12 | AR125 | WSJ | granite(mylonite) | pCC | 76.70 | 0.06 | 12.40 | 1.20 | 0.05 | < 0.10 | 0.33 | 4.10 | 4.40 | < 0.01 | < 0.010 | 0.40 | 99.64 |
| 13 | AR126 | MSJ | amphibolite | pCCanf | 57.10 | 0.81 | 16.60 | 8.00 | 0.13 | 2.70 | 9.90 | 3.10 | 0.25 | < 0.01 | 0.240 | 0.39 | 99.22 |
| 14 | AR127 | AG | granite | pCC | 73.90 | 0.34 | 14.60 | 1.90 | 0.01 | 0.56 | 0.53 | 3.90 | 2.40 | < 0.01 | < 0.010 | 1.65 | 99.79 |
| 15 | AR128 | MSJ | granite(mylonite) | pCC | 76.00 | 0.04 | 13.10 | 0.98 | 0.05 | 0.10 | 0.49 | 4.10 | 4.40 | < 0.01 | 0.018 | 0.58 | 99.86 |
| 16 | AR129 | MSJ | granite | pCC | 77.30 | 0.06 | 12.30 | 1.20 | 0.02 | < 0.10 | 0.52 | 3.90 | 4.40 | < 0.01 | < 0.010 | 0.48 | 100.18 |
| 17 | BR001 | MSJ | granite(mylonite) | pCCG | 66.50 | 0.39 | 15.70 | 3.70 | 0.05 | 1.40 | 4.00 | 4.40 | 1.60 | 0.02 | 0.110 | 1.85 | 99.72 |
| 18 | BR012 | MSJ | granite(mylonite) | pCCG | 67.60 | 0.40 | 16.10 | 3.80 | 0.05 | 1.10 | 3.20 | 4.90 | 1.20 | 0.01 | 0.120 | 1.51 | 99.99 |
| 19 | BR015 | MSJ | gabbro | gb | 50.00 | 0.51 | 13.00 | 11.10 | 0.18 | 9.80 | 10.40 | 1.40 | 1.20 | 0.12 | 0.066 | 2.20 | 99.98 |
| 20 | BR020 | MSJ | granite | pCC | 71.00 | 0.31 | 14.30 | 3.20 | 0.05 | 0.93 | 2.50 | 3.80 | 3.20 | 0.03 | 0.080 | 0.34 | 99.74 |
| 21 | BR029 | MSJ | green rock | pCCsjo | 49.00 | 1.30 | 14.80 | 13.20 | 0.18 | 5.20 | 8.60 | 2.00 | 0.03 | 0.01 | 0.200 | 5.10 | 99.62 |
| 22 | BR035 | MSJ | granite | pCC | 73.90 | 0.21 | 14.20 | 1.80 | 0.02 | 0.44 | 1.70 | 4.00 | 3.50 | < 0.01 | 0.110 | 0.24 | 100.12 |
| 23 | BR042 | MSJ | granodiorite | pCC | 54.20 | 0.49 | 12.10 | 8.70 | 0.22 | 8.50 | 10.30 | 3.10 | 0.72 | 0.05 | 0.130 | 1.31 | 99.82 |
| 24 | BR043 | MSJ | granite | pCC | 75.80 | 0.04 | 13.40 | 0.67 | 0.01 | < 0.10 | 0.22 | 4.80 | 4.30 | < 0.01 | < 0.010 | 0.28 | 99.52 |
| 25 | CR001 | MSJ | granodiorite | pCCG | 50.80 | 0.78 | 14.30 | 13.10 | 0.21 | 5.70 | 8.70 | 2.30 | 0.31 | < 0.01 | 0.095 | 2.99 | 99.29 |
| 26 | CR010 | MSJ | metagabbro | pCCps | 49.90 | 0.83 | 14.20 | 12.00 | 0.18 | 7.50 | 5.20 | 2.10 | 0.12 | 0.06 | 0.093 | 7.54 | 99.72 |
| 27 | CR016 | MSJ | granite(mylonite) | pCC | 51.40 | 0.60 | 14.20 | 11.20 | 0.18 | 8.30 | 10.90 | 2.20 | 0.08 | 0.04 | 0.087 | 0.33 | 99.52 |
| 28 | CR017 | MSJ | granite | pCC | 75.70 | 0.10 | 12.20 | 1.60 | 0.01 | 0.23 | 0.39 | 3.60 | 4.20 | < 0.01 | 0.080 | 0.56 | 98.67 |
| 29 | CR018 | MSJ | amphibolite | pCCps | 57.30 | 1.40 | 11.70 | 16.70 | 0.22 | 2.00 | 7.00 | 2.00 | 0.51 | 0.01 | 0.550 | 0.33 | 99.72 |
| 30 | CR024 | MSJ | gabbro | gb | 49.30 | 0.19 | 20.30 | 8.40 | 0.11 | 8.40 | 10.00 | 2.80 | 0.13 | 0.02 | 0.017 | 0.02 | 99.69 |

AG: The Arroyo Grande area, WSJ: The western part of the San Jose area, MSJ: The main part of the San Jose area, NSJ: The northern part of the San Jose area (wt. %)

Tab. II -3-2 Results of whole rock analysis (2)

| Ser. No. | Sample No. | Area | Rock Name | Geol.Unit | SiO ₂ | TiO ₂ | Al ₂ O ₃ | Fe ₂ O ₃ | MnO | MgO | CaO | Na ₂ O | K ₂ O | Cr ₂ O ₃ | P ₂ O ₅ | LOI | Total |
|----------|------------|------|-------------------|-----------|------------------|------------------|--------------------------------|--------------------------------|------|--------|-------|-------------------|------------------|--------------------------------|-------------------------------|--------|--------|
| 31 | CR026 | MSJ | gabbro | gb | 51.10 | 0.24 | 17.10 | 5.50 | 0.11 | 7.60 | 14.60 | 2.30 | 0.12 | 0.05 | < 0.010 | 1.23 | 99.95 |
| 32 | CR027 | MSJ | gabbro | gb | 75.70 | 0.03 | 12.90 | 1.10 | 0.06 | < 0.10 | 0.50 | 4.10 | 4.50 | 0.02 | 0.023 | 0.47 | 99.40 |
| 33 | CR029 | MSJ | granodiorite | pCC | 70.50 | 0.21 | 15.40 | 2.30 | 0.03 | 0.65 | 2.90 | 4.30 | 2.50 | 0.02 | 0.075 | 0.39 | 99.28 |
| 34 | CR036 | MSJ | granite | pCC | 76.20 | 0.14 | 12.20 | 1.60 | 0.02 | 0.16 | 0.86 | 3.30 | 4.70 | < 0.01 | 0.020 | 0.22 | 99.42 |
| 35 | CR037 | MSJ | diorite | pCC | 55.30 | 1.60 | 16.20 | 11.80 | 0.17 | 2.20 | 5.80 | 3.80 | 1.80 | < 0.01 | 0.640 | 0.41 | 99.72 |
| 36 | CR040 | MSJ | micro gabbro | dd | 53.10 | 2.20 | 12.10 | 17.00 | 0.20 | 3.10 | 7.30 | 2.60 | 1.60 | < 0.01 | 0.240 | < 0.01 | 99.44 |
| 37 | CR045 | MSJ | gabbro | pCC | 54.50 | 2.20 | 12.00 | 16.10 | 0.19 | 3.10 | 7.20 | 2.90 | 1.70 | 0.01 | 0.250 | < 0.01 | 100.15 |
| 38 | CR046 | MSJ | granite(tonalite) | pCC | 60.00 | 1.10 | 16.20 | 9.90 | 0.14 | 1.10 | 5.20 | 4.30 | 1.60 | < 0.01 | 0.340 | 0.02 | 99.90 |
| 39 | CR047 | MSJ | granite | pCC | 64.70 | 0.60 | 15.40 | 5.70 | 0.08 | 2.30 | 4.70 | 4.00 | 1.80 | < 0.01 | 0.210 | 0.72 | 100.21 |
| 40 | CR048 | MSJ | amphibolite | dd | 49.70 | 0.94 | 14.80 | 14.00 | 0.20 | 7.60 | 11.20 | 1.00 | 0.04 | 0.03 | 0.070 | 0.63 | 100.21 |
| 41 | CR051 | MSJ | granite | pCC | 54.20 | 0.52 | 19.40 | 7.20 | 0.11 | 4.80 | 8.70 | 3.50 | 0.39 | 0.01 | 0.140 | 1.00 | 99.97 |
| 42 | CR055 | MSJ | granite | pCCG | 71.10 | 0.26 | 14.50 | 2.90 | 0.06 | 0.48 | 1.40 | 4.60 | 4.10 | < 0.01 | 0.130 | 0.49 | 100.02 |
| 43 | CR057 | MSJ | granite | pCCG | 69.90 | 0.29 | 15.10 | 3.00 | 0.05 | 0.56 | 1.70 | 4.80 | 3.90 | < 0.01 | 0.120 | 0.44 | 99.86 |
| 44 | CR059 | MSJ | granite | pCC | 77.40 | 0.05 | 12.50 | 0.80 | 0.02 | < 0.10 | 0.77 | 3.90 | 4.10 | < 0.01 | 0.021 | 0.23 | 99.79 |
| 45 | CR060 | MSJ | granite | pCCG | 75.20 | 0.11 | 14.10 | 1.20 | 0.03 | 0.25 | 1.50 | 3.80 | 3.80 | < 0.01 | 0.093 | 0.43 | 100.51 |
| 46 | CR061 | MSJ | granite(mylonite) | pCCcb | 77.30 | 0.06 | 12.90 | 0.68 | 0.02 | < 0.10 | 0.61 | 4.10 | 4.00 | < 0.01 | 0.018 | 0.20 | 99.89 |
| 47 | CR125 | WSJ | granodiorite | pCC | 53.80 | 0.21 | 20.30 | 5.70 | 0.10 | 4.60 | 11.60 | 2.80 | 0.21 | < 0.01 | 0.025 | 0.80 | 100.15 |
| 48 | CR126 | WSJ | gabbro | pCCG | 52.00 | 0.17 | 21.10 | 6.60 | 0.12 | 5.10 | 11.60 | 2.70 | 0.17 | < 0.01 | < 0.010 | 0.29 | 99.85 |
| 49 | DR028 | MSJ | porphyry | pCCps | 76.30 | 0.02 | 13.90 | 0.87 | 0.01 | < 0.10 | 0.10 | 3.70 | 4.40 | < 0.01 | 0.026 | 0.73 | 100.06 |
| 50 | ER003 | MSJ | quartz schist | pCCps | 57.70 | 0.61 | 14.80 | 6.30 | 0.08 | 3.20 | 5.90 | 0.97 | 1.80 | < 0.01 | 0.150 | 7.77 | 99.28 |
| 51 | ER030 | MSJ | granite | pCCG | 64.50 | 0.60 | 15.80 | 5.80 | 0.09 | 2.60 | 5.10 | 4.00 | 1.20 | < 0.01 | 0.160 | 0.53 | 100.38 |
| 52 | ER051 | MSJ | granodiorite | pCCG | 66.50 | 0.40 | 16.30 | 3.80 | 0.05 | 1.40 | 4.30 | 4.80 | 1.30 | < 0.01 | 0.120 | 1.20 | 100.17 |
| 53 | ER058 | MSJ | gabbro | pCCsjo | 41.70 | 2.60 | 17.30 | 18.90 | 0.23 | 7.00 | 8.10 | 1.50 | 2.30 | 0.07 | 0.490 | 0.50 | 100.69 |
| 54 | ER076 | AG | granite | pCC | 72.30 | 0.22 | 14.90 | 1.90 | 0.03 | 0.49 | 2.30 | 4.10 | 2.80 | 0.03 | 0.083 | 0.39 | 99.54 |
| 55 | ER077 | AG | meta rhyolite | pCCag | 75.50 | 0.03 | 13.50 | 1.50 | 0.06 | 0.10 | 0.70 | 4.10 | 3.60 | 0.02 | 0.048 | 0.39 | 99.55 |
| 56 | FR008 | MSJ | granite | pCC | 61.90 | 0.69 | 16.40 | 6.40 | 0.09 | 2.60 | 5.20 | 4.10 | 1.50 | < 0.01 | 0.200 | 0.67 | 99.75 |
| 57 | FR010 | MSJ | granite | pCCbc | 67.00 | 0.56 | 15.60 | 5.90 | 0.26 | 2.40 | 1.60 | 2.10 | 2.20 | 0.03 | 0.140 | 1.71 | 99.50 |
| 58 | FR011 | MSJ | granite(mylonite) | pCC | 72.80 | 0.15 | 14.10 | 1.80 | 0.04 | 0.37 | 2.00 | 3.80 | 3.50 | < 0.01 | 0.150 | 0.52 | 99.23 |
| 59 | FR012 | MSJ | granite | pCC | 74.40 | 0.14 | 14.30 | 1.60 | 0.05 | 0.31 | 1.80 | 4.40 | 2.70 | < 0.01 | 0.066 | 0.72 | 100.49 |
| 60 | GR021 | MSJ | gabbro | pCCG | 53.00 | 0.71 | 18.20 | 7.00 | 0.11 | 4.90 | 8.70 | 3.50 | 0.88 | 0.03 | 0.330 | 1.87 | 99.23 |
| 61 | GR055 | NSJ | granodiorite | pCCG | 68.20 | 0.32 | 16.40 | 3.10 | 0.06 | 1.10 | 3.70 | 4.90 | 1.50 | 0.03 | 0.110 | 0.56 | 99.98 |

AG: The Arroyo Grande area, WSJ: The western part of the San Jose area, MSJ: The main part of the San Jose area, NSJ: The northern part of the San Jose area (wt. %)

Tab. II -3-3 Results of radiometric dating

| Ser. No. | Sample No. | Area | Rock Name | Geol. Unit | Sample Type | Potassium (K wt%) | Rad. ⁴⁰ Ar (10 ⁻⁶ cc/g) | K-Ar age (Ma) | Air Cont. (%) |
|----------|------------|---------------------------------------|-------------|------------|-------------|-------------------|---|---------------|---------------|
| 1 | AR125 | The western part of the San Jose area | granite | pCC | whole rock | 3.12 ± 2 | 34000 ± 1700 | 1690 ± 120 | 1.4 |
| 2 | AR126 | The main part of the San Jose area | amphibolite | pCCanf | whole rock | 0.17 ± 10 | 2420 ± 120 | 2000 ± 280 | 1.8 |
| 3 | AR127 | The Arroyo Grande area | granite | pCC | whole rock | 1.76 ± 2 | 24700 ± 1200 | 1980 ± 130 | 1.9 |
| 4 | AR128 | The main part of the San Jose area | granite | pCC | whole rock | 4.09 ± 2 | 28200 ± 1400 | 1240 ± 100 | 0.9 |
| 5 | AR129 | The main part of the San Jose area | granite | pCC | whole rock | 3.41 ± 2 | 3900 ± 2000 | 1750 ± 120 | 0.9 |
| 6 | BR001 | The main part of the San Jose area | granite | pCCG | whole rock | 1.16 ± 2 | 16000 ± 800 | 1960 ± 140 | 1.0 |

$\lambda \epsilon = 0.581 \times 10^{10} / \text{year}$, $\lambda \beta = 4.962 \times 10^{10} / \text{year}$
⁴⁰K/K=0.01167 atom%

Tab. II -3-4 Results of X-ray diffractive analysis (1)

| Ser. No. | Sample No. | Area | Rock Name | Geol. Unit | Detected Minerals | | | | | | | | | | | | | | | |
|----------|------------|------------------------------------|---------------|------------|-------------------|------------|--------|-------------------|----------|----------|---------|-----------|------------|---------|--------|----------|----------|--|--|---|
| | | | | | quartz | K-feldspar | albite | chlorite/smectite | chlorite | sericite | calcite | muscovite | hornblende | epidote | pyrite | hematite | goethite | | | |
| 1 | AR026 | The main part of the San Jose area | green schist | pCCps | ◎ | | | ◎ | | | | | | | | | △ | | | |
| 2 | AR032 | The main part of the San Jose area | green schist | pCCps | ◎ | | | ◎ | | tr | | | | | | | | | | |
| 3 | AR039 | The main part of the San Jose area | green schist | pCCps | ◎ | | | ◎ | | tr | ▲ | | | | | | ▲ | | | |
| 4 | AR041 | The main part of the San Jose area | green rock | pCCps | ◎ | | | ◎ | | | ▲ | | | | | | | | | |
| 5 | AR047 | The main part of the San Jose area | metabasalt | pCCps | ◎ | | | ◎ | | | | | | | | ◎ | △ | | | |
| 6 | AR054 | The main part of the San Jose area | metabasalt | pCCps | ○ | | | ◎ | | | | | | | | ◎ | ○ | | | |
| 7 | AR120 | The main part of the San Jose area | quartz vein | pCCG | ◎ | | | △ | | | | | | | | | | | | |
| 8 | BR030 | The main part of the San Jose area | green rock | pCCsjo | ◎ | | | ◎ | | | | | | | | | | | | |
| 9 | BR031 | The main part of the San Jose area | quartz schist | pCCsjo | ◎ | | | ◎ | | | | | | | | | | | | |
| 10 | BR032 | The main part of the San Jose area | green rock | pCCsjo | ◎ | | | ○ | | | | | | | | | | | | |
| 11 | BR033 | The main part of the San Jose area | black schist | pCCsjo | ◎ | | | ○ | ◎ | | | | | | | | | | | |
| 12 | BR034 | The main part of the San Jose area | green rock | pCCsjo | ◎ | | | ◎ | | | ▲ | | | | | ◎ | | | | |
| 13 | BR036 | The main part of the San Jose area | green schist | pCCsjo | ◎ | | | | | | | | | | | | | | | |
| 14 | BR037 | The main part of the San Jose area | green schist | pCCsjo | ◎ | | | ◎ | | | | | | | | ◎ | | | | |
| 15 | BR038 | The main part of the San Jose area | green schist | pCCps | ◎ | | | ◎ | | | | | | | | | | | | ○ |
| 16 | BR039 | The main part of the San Jose area | green schist | pCCps | | | | ◎ | | | | | | | | | | | | |
| 17 | BR040 | The main part of the San Jose area | green schist | pCCps | ◎ | | | ◎ | | | | | | | | | | | | ○ |
| 18 | BR041 | The main part of the San Jose area | green schist | pCCps | ◎ | | | △ | | | | | | | | | | | | △ |
| 19 | BR055 | The Arroyo Grande area | green schist | pCCag | ◎ | | | ○ | | | | | | | | | | | | |
| 20 | CR019 | The main part of the San Jose area | black chert | pCCps | ◎ | | | | | | | | | | | | | | | △ |

◎: >1000 cps, ○: 500-1000 cps, △: 200-500 cps, ▲: 100-200 cps, tr: <100 cps

Tab. II -3-4 Results of X-ray diffractive analysis (2)

| Ser. No. | Sample No. | Area | Rock Name | Geol. Unit | Detected Minerals | | | | | | | | | | | | | | |
|----------|------------|---------------------------------------|--------------|------------|-------------------|------------|--------|-------------------|----------|----------|---------|-----------|------------|---------|--------|----------|----------|---|---|
| | | | | | quartz | K-feldspar | albite | chlorite/smectite | chlorite | sericite | calcite | muscovite | hornblende | epidote | pyrite | hematite | goethite | | |
| 21 | CR048 | The main part of the San Jose area | metadiorite | pCC | Δ | | ○ | tr | | | | | ⊙ | | | | | | |
| 22 | CR123 | The western part of the San Jose area | granite | pCCG | | | ⊙ | Δ | | | | | ⊙ | | | | | | |
| 23 | DR037 | The main part of the San Jose area | quartz vein | pCCsjo | ⊙ | | | | | | | | | | | | | | Δ |
| 24 | DR041 | The main part of the San Jose area | slate | pCCps | ⊙ | | ○ | ○ | | ○ | | | | | | | | ▲ | |
| 25 | ER029 | The main part of the San Jose area | green schist | pCCsjo | ⊙ | | Δ | ⊙ | | | | | | | ⊙ | | | | |
| 26 | GR013 | The main part of the San Jose area | green schist | pCCsjo | ⊙ | | ⊙ | ⊙ | | ○ | | | | | | | | | |
| 27 | GR015 | The main part of the San Jose area | green schist | pCCps | ⊙ | | ○ | ⊙ | | ○ | | | | ⊙ | | | | | |
| 28 | GR016 | The main part of the San Jose area | metabasalt | pCCps | ⊙ | | ⊙ | | | ⊙ | | | | | | | | | |
| 29 | GR018 | The main part of the San Jose area | green schist | pCCps | ⊙ | | ⊙ | ⊙ | | | | | | | | | | ▲ | |
| 30 | GR038 | The Arroyo Grande area | quartz vein | pCCag | ⊙ | | ⊙ | | | | | | ⊙ | | | | | | |
| 31 | JR025 | The Arroyo Grande area | green schist | pCCag | ⊙ | | ⊙ | ⊙ | | | | | | | ○ | | | | Δ |

⊙: >1000 cps, ○: 500-1000 cps, Δ: 200-500 cps, ▲: 100-200 cps, tr: <100 cps

Tab. II -3-5 Description of polished sections (2)

| Ser. No. | Sample No. | Area | Rock Name | Geol. Unit | Description | Phenocrysts, crystals | | | | | | | | | | | Gangue Minerals | | | | | | | | | | | | | |
|----------|------------|------|-------------------------|------------|---|-----------------------|----------|----------|----------|-----------|----------------|------------|-----------|-----------|--------|----------------|-----------------|--------|-----------------|----------|----------|---|--|--|--|---|--|--|--|--|
| | | | | | | pyrite | goethite | hematite | limonite | magnetite | chalcocopyrite | chalcocite | covellite | shalerite | galena | rutile/anatase | quartz | zircon | phyllosilicates | titanite | Ilmenite | | | | | | | | | |
| 21 | DR004 | MSJ | green schist | pCCsjo | qz: 20-1000 μ m ϕ , py: 200-900 μ m ϕ | ● | | | | | | | | | | | | | | | | ○ | | | | ? | | | | |
| 22 | DR006 | MSJ | microgabbro | gb | py: 20-140 μ m ϕ , cp: 25-90 μ m ϕ | ● | | | | | | | | | | | | | | | | ● | | | | | | | | |
| 23 | DR027 | MSJ | quartz vein | pCCcb | py: 5-10 μ m ϕ | . | | | | | | | | | | | | | | | | | | | | | | | | |
| 24 | DR031 | MSJ | quartz-sericitic schist | pCCG | py: 10-20 μ m ϕ | . | | | | | | | | | | | | | | | | | | | | | | | | |
| 25 | DR037 | MSJ | quartz vein | pCCsjo | py: 5-20 μ m ϕ within siliceous part | . | | | | | | | | | | | | | | | | | | | | | | | | |
| 26 | DR040 | MSJ | quartz vein | pCCps | py: 2-5 μ m ϕ | . | | | | | | | | | | | | | | | | | | | | | | | | |
| 27 | ER005 | MSJ | quartz vein | pCCps | with limonite | . | | | | | | | | | | | | | | | | | | | | | | | | |
| 28 | ER013 | MSJ | quartz vein | pCCcb | py: a few mm ϕ | ● | | | | | | | | | | | | | | | | | | | | | | | | |
| 29 | ER039 | MSJ | magnetite | pCCcb | magnetite, hematite, limonite | | | | | | | | | | | | | | | | | | | | | | | | | |
| 30 | ER040 | MSJ | quartz vein | pCCcb | py: 1-5 μ m ϕ | . | | | | | | | | | | | | | | | | | | | | | | | | |
| 31 | ER087 | AG | quartz vein | pCC | limonite along fracture | | | | | | | | | | | | | | | | | | | | | | | | | |
| 32 | FR006 | MSJ | quartz vein | pCCps | py: 5-8 μ m ϕ | . | | | | | | | | | | | | | | | | | | | | | | | | |
| 33 | GR 008 | MSJ | quartz vein | pCCsjo | py: 2-5 μ m ϕ | . | | | | | | | | | | | | | | | | | | | | | | | | |
| 34 | GR 012 | MSJ | green schist | pCC | magnetite & hematite: 100-500 μ m ϕ | | | | | | | | | | | | | | | | | | | | | | | | | |
| 35 | GR 018 | MSJ | green schist | pCCps | porphyroblast of qz & magnetite: 100-700 μ m ϕ | | | | | | | | | | | | | | | | | | | | | | | | | |
| 36 | GR 019 | MSJ | metabasalt | pCCps | hematite: 10-45 μ m ϕ | | | | | | | | | | | | | | | | | | | | | | | | | |
| 37 | JR001 | MSJ | quartz vein | pCCps | fracture without sulfide | | | | | | | | | | | | | | | | | | | | | | | | | |
| 38 | JR028 | AG | quartz vein | pCCag | py within qt: 5-10 μ m ϕ | . | | | | | | | | | | | | | | | | | | | | | | | | |

AG: The Arroyo Grande area, WSJ: The western part of the San Jose area, MSJ: The main part of the San Jose area

●: abundant, ○: common, ●: a little, •: rare

Tab. II -3-6 Homogenization temperature and salinity of fluid inclusions

| Set. No. | Sample No. | Area | Mineral Showings | Rock Name | Geol. Unit | Temperature (°C) | | | Salinity (%) |
|----------|------------|------------------------------------|------------------|-------------|------------|------------------|---------------|---------|--------------|
| | | | | | | Number | Range | Average | |
| 1 | AR027 | The main part of the San Jose area | Arroyo Charruzo | quartz vein | pCCps | 30 | 102.3 - 216.6 | 162.1 | 13.6 |
| 2 | AR036 | The main part of the San Jose area | Arroyo Charruzo | quartz vein | pCCps | 30 | 129.0 - 192.6 | 165.2 | 4.8 |
| 3 | CR032 | The main part of the San Jose area | Arroy del Medio | quartz vein | pCCps | 30 | 122.6 - 250.5 | 155.8 | >23 |
| 4 | CR056 | The main part of the San Jose area | Tala II | quartz vein | pCCG | 20 | 141.7 - 321.3 | 227.0 | 4.3 |
| 5 | CR058 | The main part of the San Jose area | Tala II | quartz vein | pCCG | 30 | 115.8 - 267.4 | 154.3 | 18.0 |
| 6 | DR025 | The main part of the San Jose area | Mahoma | quartz vein | pCCps | 20 | 157.1 - 357.5 | 247.5 | 20.0 |
| 7 | DR027 | The main part of the San Jose area | Mahoma | quartz vein | pCCcb | 20 | 150.9 - 270.3 | 211.5 | 21.2 |
| 8 | ER017 | The main part of the San Jose area | Arroyo Charruzo | quartz vein | pCCsjo | 30 | 85.6 - 263.2 | 166.0 | 31 |
| 9 | ER023 | The main part of the San Jose area | Arroyo Charruzo | quartz vein | pCCsjo | 30 | 100.2 - 223.2 | 157.7 | 32 |
| 10 | ER027 | The main part of the San Jose area | Arroyo Charruzo | quartz vein | pCCsjo | 30 | 133.6 - 223.1 | 184.3 | 7.2 |
| 11 | ER037 | The main part of the San Jose area | Tala II | quartz vein | pCCG | 20 | 164.5 - 334.2 | 237.1 | 16.9 |
| 12 | ER084 | The Arroyo Grande area | Rio Negro II | quartz vein | pCC | 30 | 141.7 - 447.7 | 322.2 | 35 |
| 13 | ER093 | The Arroyo Grande area | Rio Negro II | quartz vein | pCCag | 30 | 140.2 - 258.0 | 196.7 | 4.2 |
| 14 | JR002 | The main part of the San Jose area | Tala II | quartz vein | pCCps | 20 | 99.2 - 278.5 | 148.7 | 20.1 |